

5-15-2018

Design & Delivery of Automated Winston-Lutz Test for Isocentric & Off-Axis Delivery Stability Utilizing Truebeam Developer Mode & Electronic Portal Imaging Device

Mahmoud Mohammad Yaqoub

Follow this and additional works at: <https://digitalscholarship.unlv.edu/thesesdissertations>



Part of the [Biomechanical Engineering Commons](#), [Biomedical Commons](#), [Biomedical Devices and Instrumentation Commons](#), [Medicine and Health Sciences Commons](#), and the [Nuclear Commons](#)

Repository Citation

Yaqoub, Mahmoud Mohammad, "Design & Delivery of Automated Winston-Lutz Test for Isocentric & Off-Axis Delivery Stability Utilizing Truebeam Developer Mode & Electronic Portal Imaging Device" (2018).

UNLV Theses, Dissertations, Professional Papers, and Capstones. 3349.

<http://dx.doi.org/10.34917/13568805>

This Thesis is protected by copyright and/or related rights. It has been brought to you by Digital Scholarship@UNLV with permission from the rights-holder(s). You are free to use this Thesis in any way that is permitted by the copyright and related rights legislation that applies to your use. For other uses you need to obtain permission from the rights-holder(s) directly, unless additional rights are indicated by a Creative Commons license in the record and/or on the work itself.

This Thesis has been accepted for inclusion in UNLV Theses, Dissertations, Professional Papers, and Capstones by an authorized administrator of Digital Scholarship@UNLV. For more information, please contact digitalscholarship@unlv.edu.

DESIGN & DELIVERY OF AUTOMATED WINSTON-LUTZ TEST FOR ISOCENTRIC &
OFF-AXIS DELIVERY STABILITY UTILIZING TRUEBEAM DEVELOPER MODE &
ELECTRONIC PORTAL IMAGING DEVICE

By

Mahmoud Yaqoub

Bachelor of Science - Applied physics/Nuclear and Radiation Technique
Jordan University of Science and Technology
2001

Master of Science - Applied Physics
Texas Tech University
2013

Master of Science - Electrical Engineering
Northern Illinois University
2016

A thesis submitted in partial fulfillment
of the requirements for the

Master of Science – Health Physics

Department of Health Physics and Diagnostic Sciences
School of Allied Health Sciences
Division of Health Sciences
The Graduate College

University of Nevada, Las Vegas
May 2018



Thesis Approval

The Graduate College
The University of Nevada, Las Vegas

April 6, 2018

This thesis prepared by

Mahmoud Yaqoub

entitled

Design & Delivery of Automated Winston-Lutz Test for Isocentric & Off-Axis Delivery
Stability Utilizing TrueBeam Developer Mode & Electronic Portal Imaging Device

is approved in partial fulfillment of the requirements for the degree of

Master of Science – Health Physics
Department of Health Physics and Diagnostic Sciences

Yu Kuang, Ph.D.
Examination Committee Chair

Kathryn Hausbeck Korgan, Ph.D.
Graduate College Interim Dean

Matthew Schmidt, Ph.D.
Examination Committee Member

Steen Madsen, Ph.D.
Examination Committee Member

Szu-Ping Lee, Ph.D.
Graduate College Faculty Representative

ABSTRACT

The uncertainties in treatment delivery cannot be ignored in radiation therapy. Thus, the quality assurance QA tests are very important task of the medical physicist in clinical practice. Assuring the coincidence between the mechanical isocenter of the Linear Accelerator (LINAC) and its radiation beams isocenter is one of the most important qualities need to be tested, and the Winston Lust (WL) test is the most popular technique to perform this task, especially for the treatment modalities which need high precision in beam delivery such as the stereotactic radiosurgery/stereotactic body radiotherapy (SRS/SBRT). The linear accelerator-based SRS/SBRT is a well-established method in radiation therapy. There is a recent interest in the single-isocenter technique to treat multiple lesions. However, there is a shortage in studying the accuracy of this technique, to verify the mechanical field center coincidence with the radiation field center when both are off-isocenter.

In the first part of this work, an automatic WL was designed in purpose to be used in routine QA tasks. More images were acquired at broader combinations of the gantry and couch rotation angles. The 20 images automated WL needed less than 13 min to be performed, where the regular manual WL test for 8 images required an average time of 29 minutes. Also, the Automated WL only needed one-time setup and no need to go inside the treatment room between each image acquisition to change the setup, this decreased the chances of any possible errors.

In the second part, an innovative Python code was developed to extract the MultiLeaves Collimator MLC positions at the cardinal angles of a conformal arc treatment plan, which was designed to treat multiple lesions located at distances 2, 4, 6, 8 cm off-isocenter, and then were exported as Digital Imaging and Communication in Medicine format (DICOM) file to Python. Out of these DICOM treatment planning files, Python would generate an eXtensible Markup

Language (XML) file of the automated WL test with all the collimating leaves positions presented in the treatment planning, to acquire images at the cardinal angles for each off-isocenter displacement. After feeding the generated XML files of the automated WL test to the developer mode of the True Beam LINAC, images were acquired at the cardinal angles to quantify the inaccuracy of the isocenter of the beam in targeting the center of the lesion, which was 2, 4, 6 and 8 cm off-isocenter of the LINAC machine. The resulted measurements indicate that the single isocenter multiple lesions technique complies with the recommended maximum tolerance for the LINAC-based SRS/SBRT treatment. Finally, the pitch and roll weight compensation of the six Degree of Freedom (6DoF) couch of the Varian TrueBeam LINAC was tested. The robotic couch adjusted the pitch angle to adjust the coordinate of the target vertically at every off-isocenter displacement, which made the positioning of the target in the middle of the beam possible more accurate.

ACKNOWLEDGMENT

I would first like to thank my thesis advisory committee, Dr. Yu Kuang-Chair, Dr. Steen Madsen, Dr. Szu-Ping Lee and Mr. Matthew Schmidt. The door to Mr. Schmidt was always open whenever I ran into a trouble spot or had a question about my research or writing. He consistently allowed this thesis to be my own work but steered me in the right the direction whenever he thought I needed it.

I would like to thank the Department of Health Physics and Diagnostic Sciences, faculty and staff at the University of Nevada, Las Vegas for their help and support during my study and research.

I also would like to thank Varian Medical Systems, Las Vegas Nevada, for providing the necessary equipment, labs and technical and theoretical support for my research. In addition to the professional friendly research environment. Without any doubt my experience there is unforgettable.

Last but by no means least, I must express my very profound gratitude to my father, my wife and my children for their patience and sacrifice. They have provided me with unfailing support and continuous encouragement throughout my years of study and through the process of researching and writing this thesis. This accomplishment would not have been possible without them.

To my role model, my father.

To the memory of my mother.

To my best team, My wife and kids.

TABLE OF CONTENTS

ABSTRACT.....	iii
ACKNOWLEDGMENT.....	v
TABLE OF CONTENTS.....	vii
LIST OF FIGURES	viii
CHAPTER 1: INTRODUCTION	1
1.1 Radiation Therapy.....	1
1.2 The TrueBeam Linear Accelerator.....	3
1.2.1 General Information	3
1.2.2 Multi-Leaf Collimators (MLC's).....	4
1.2.3 Electronic portal imaging devices (EPIDs)	5
1.2.4 TrueBeam Developer Mode	6
1.3 Stereotactic Radiosurgery SRS and Stereotactic Body Radiation Therapy SBRT	8
1.4 Single Isocenter-Multiple Lesion LINAC-Based SRS/SBRS.....	9
1.5 Quality Assurance	10
1.6 Winston-Lutz Test.....	11
1.7 Significance of Study and Objectives	12
CHAPTER 2: MATERIALS AND METHOD.....	14
2.1 Experiment's Material.....	14
2.2 EPID Quality Assurance	15
2.3 Automated Winston Lutz Test	16
2.4 Automated off-Isocenter Winston-Lutz	17
2.5 Analyzing the Images.....	23
CHAPTER 3: RESULTS.....	25
CHAPTER 4: DISCUSSION.....	33
CHAPTER 5: CONCLUSION & RECOMMENDATIONS.....	36
APPENDICES	38
Appendix 1: The XML script for 20 images WL test	38
Appendix 2: The XML script from Python code for the off-isocenter automated WL test.....	48
References.....	53
Curriculum Vitae	56

LIST OF FIGURES

Figure 1: Diagram showing the parts and components of the medical LINAC [6].....	4
Figure 2: Workflow of developing and delivering an XML beam on TrueBeam Developer mode [10].....	7
Figure 3: The trajectory function and control points [10].....	7
Figure 4: The IsoCal system	15
Figure 5: WL test set up on the TrueBeam LINAC using circular drill hole collimator.....	16
Figure 6: The BB phantom.	17
Figure 7: Eclipse conformal arc plan for different PTVs	18
Figure 8: The differences between Varian and the standard system.	19
Figure 9: Centering the BB phantom in the light field	20
Figure 10: The work flow of the off-isocenter WL test.....	21
Figure 11: The robotic 6DoF couch.....	22
Figure 12: The weight-loaded couch to mimic the clinical situation.....	22
Figure 13: The coordinate system used in Pylinac	24
Figure 14: The couch and gantry angle configuration versus the control points for the 20 images WL test.....	25
Figure 15: An example of selected part of the results report generated by Pylinac [25].....	26
Figure 16: The x, y and z direction of the maximum shift of the BB from the isocenter.....	28
Figure 17: The x, y and z direction of the maximum shift of the BB from the isocenter.....	28
Figure 18: The maximum and median 2D shifts between the CAX and the BB, for different off-isocenter displacement.	29

Figure 19: The maximum 2D shifts between the CAX and the BB, for different off-isocenter displacements, versus the gantry angle..... 30

Figure 20: The difference in the x, y and z direction of the shift of the BB from the isocenter between the loaded and unloaded couch..... 31

Figure 21: The maximum shift of the BB from the CAX versus the gantry angle, when the couch is unloaded 32

Figure 22: on the left, the transverse, frontal and sagittal views of the PTV. On the right, zoomed view of the transverse view showing the shift between the reference point and the center of the PTV..... 35

CHAPTER 1:

INTRODUCTION

1.1 Radiation Therapy

Cancer is considered among the main cause of death around the world [1]. According to the International Agency for Research on Cancer (IARC) in 2012, cancer has killed 8.2 million people, and there are 14.1 million new cases yearly reported worldwide [2]. However, during the past decade, there was considerable progress toward understanding the earlier hallmarks of cancer and early detection of this disease and treatment modalities. Radiation therapy, along with the chemotherapy and surgery, is used to treat cancer depending on the cancer type, stage, size and its position [2].

The modern advances in imaging techniques and radiation treatment machines, presented in the improvement in X-ray production, computerized treatment planning systems and treatment delivery, as well as improved understanding of the radiobiology of radiation therapy, have made many cancers controllable and curable [1]. In the United States, in 2004, 1 million out of 1.4 million people who were diagnosed with cancer, was treated with radiation. In general, the radiation therapy used to treat 50% of all cancer patients during their course of illness, 60 % of whom were treated with curative intent. Radiation therapy is considered as highly cost-effective; only 5% of the total cost of cancer care goes to radiation therapy [3].

At the beginning of the radiation therapy, before 1950, the kilovoltage x-rays were used for external radiotherapy, which was up to 300 kVp. Later higher energy radiations were used such as the cobalt-60 radiation and higher energy machines. Eventually, the conventional kilovoltage machine started to demise gradually although it is still used today for limited purposes such as superficial skin lesions. A continuous development in manufacturing the high energy machine started the era of the megavoltage beams for external radiotherapy [4].

X- or gamma ray beam are used widely in radiation therapy, this is because the interaction of their beam photons with human body tissues can destroy the tumor cells reproductive capacity. The mechanism of the interaction solely based on the transferred energy from the beam photons to the medium; this will cause electrons of the atoms of the absorbing medium to be ejected from atoms. These electrons are moving with high speed and energy, which is sufficient to produce ionization and excitation of the atoms along their path in the tumor tissues. If the deposited energy in the cancerous cell is sufficient, then it will destroy the cell and its component, such as the DNA. Eventually, in the end, the cancerous cell will lose its power to reproduce and proliferate and die. However, this sufficient energy is a small portion of the absorbed one; the majority of the absorbed energy is converted to heat which is not sufficient to produce the significant biological effect. This situation is desired when the ionizing radiation has to pass through a healthy tissue in order to be delivered to the lesion [5].

The main goal of radiation therapy is to attain the highest cure rate probability and the least morbidity. This goal can be achieved by maximizing the radiation dose to abnormal cancer cells while minimizing it to the normal cell which is in the path of radiation or adjacent to cancer cells. Fortunately, although the radiation damages both healthy cells and cancer cells, but healthy cells, usually, have more capability to repair themselves at a faster rate, so they can retain their

normal functions than the cancer cells. In general, cancer cells have less efficiency than healthy cells in repairing the radiation damage. After irradiation, cancer cells significantly have less chance to survive than the normal cells.

Since the beginning of radiation therapy, different techniques were introduced and improved. External beam radiotherapy is wide and it contains different radiotherapy techniques. Such as intensity modulated radiation therapy IMRT, volumetric arc therapy VMAT or Rapid Arc, image-guided radiation therapy IGRT, stereotactic radiosurgery SRS and stereotactic body radiation therapy SBRT. This work is dealing with the last two techniques, SRS and SBRT.

1.2 The TrueBeam Linear Accelerator

1.2.1 General Information

A linear accelerator (LINAC) is an external beam radiation generator; it became the most widely used radiation source in modern radiotherapy. It offers excellent versatility for use in radiotherapy through isocentric mounting due to its compact and efficient design [6]. In the LINAC, the charged particles, the electrons, are accelerated in a linear path inside the accelerator waveguide, the charged particles within this structure are driven by high radio frequency electromagnetic waves to desired energies, and provides either electron or megavoltage X-ray therapy with a wide range of energies. The accelerated electrons then allowed to collide with a heavy metal target to generate high energy X-Rays (Photons) [6]. The generated high energy X-Rays then will be directed accurately to the tumor inside the patient's body. The radiation beam is shaped within the LINAC head to conform to the shape of the tumor. The gantry rotates 360 degrees around the mechanical center point, the isocenter. It contains three components: the electron gun, the accelerator structure, and the treatment head. The treatment head contains the

treatment beam shaping and monitoring components. This will provide the capability to deliver the radiation beam to the tumor from any angle by rotating the gantry and the treatment couch.

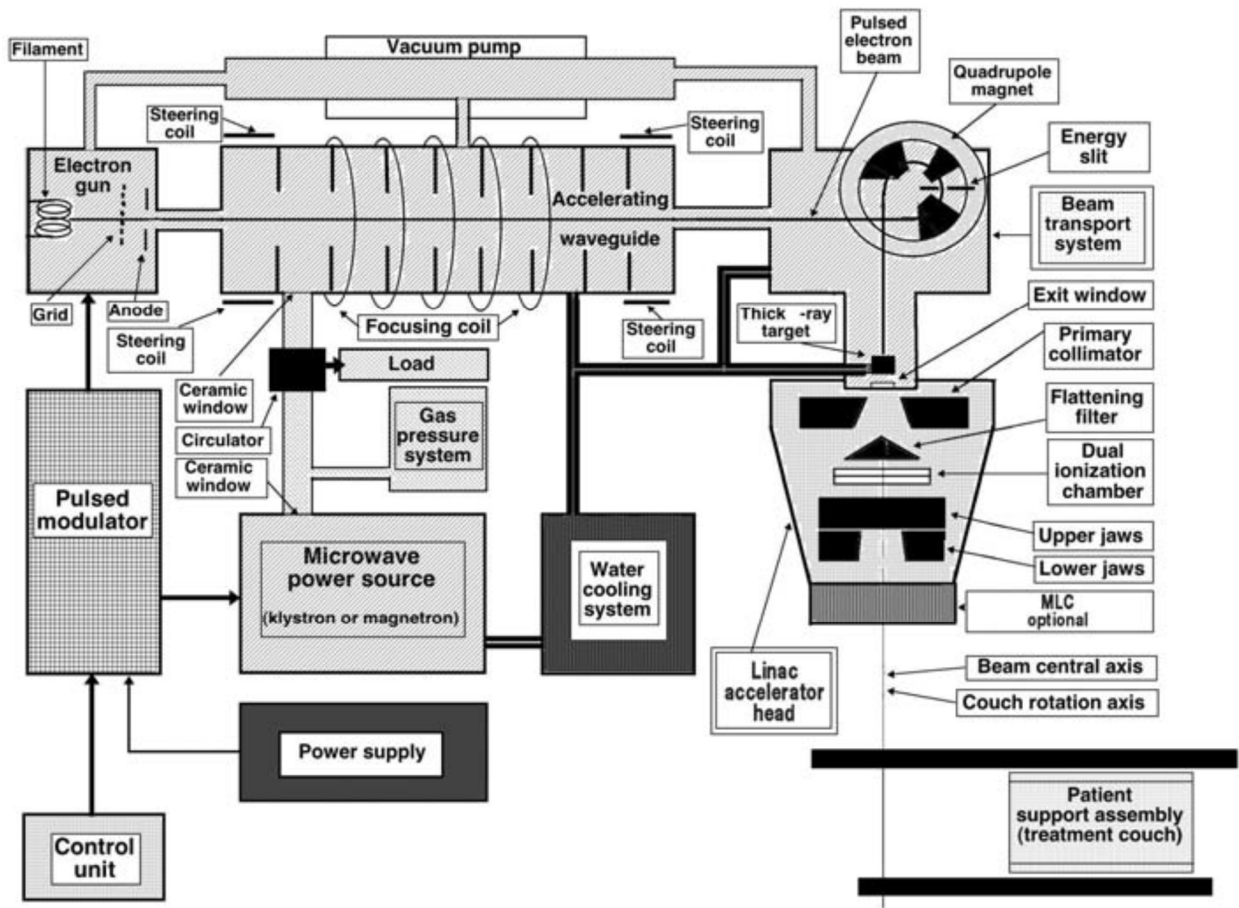


Figure 1: Diagram showing the parts and components of the medical LINAC [6].

1.2.2 Multi-Leaf Collimators (MLC's)

The radiation beams are collimated by adjusting the upper and lower collimator jaws made of Tungsten or Lead. The jaws can define a rectangular shaped beam up to 40 cm by 40 cm for X-ray beams. Additional shaping is required if the treatment volume is not rectangular. Then tungsten blocks are attached to the treatment head, under the standard collimating system, called

Multi-Leaf Collimators (MLC's). MLC's are heavy metal, field-shaping device used to spare normal tissue and direct the radiation dose to the lesion by adjusting its multipole independent movable leaves, to create a custom blocks to conform the radiation beam to the lesion shape. Typical MLCs have 40 to 120 leaves, arranged in pairs. By moving and controlling this a large number of narrow, closely abutting individual leaves, one can generate almost any desired field shape.

In TrueBeam machine from Varian, there are 120 leaves, over a 40x22 cm field. The central 8 cm of the field has 2.5 mm leaf width, where the outer 14cm of the field have 5mm leaf width. Each leaf can be driven separately as it going to be shown later.

1.2.3 Electronic portal imaging devices (EPIDs)

Electronic Portal Imaging Devices (EPIDs) measures the intensity of the transmitted x-ray during the treatment session. There is a radiation port attached to the gantry generating the X-ray radiation, which its transmitted part will fall perpendicular to the detector plate. Then the detected radiation intensity will be converted to an electronic signal, which will be processed to produce a two-dimensional (2D) digital radiographic image. This image usually produced to verify the correct beam placement in relation to the patient's anatomy [7].

Electronic portal imaging devices (EPIDs) have gradually replaced films for patient positioning, QA tests on linear accelerators, and treatment dosimetry verification [8]. EPID image quality and QA tests based on EPID can be degraded and become inaccurate due to different mechanical components, such as the gantry motion itself, the supporting arm and its joints, the fastener and the gear belt. Hence, they must be tested routinely for geometric accuracy, image quality, and operational safety. One way to test the geometric accuracy is the Isocenter calibration (IsoCal)

geometric calibration system. In the IsoCal calibration process, MV images are taken for the phantom at different gantry angles, see figure 4, then the IsoCal software can recognize the treatment isocenter and match it to the MV imaging center, the offset between the two isocenters will be calculated for each gantry angle. based on this calculation, the system will compile a correction file, which the True Beam will use it to apply any necessary physical corrections automatically to the imaging panel during image acquisition. [9].

1.2.4 TrueBeam Developer Mode

Within the TrueBeam control system architecture, the application home screen includes modules for Treatment, Service, Developer Mode and others. The Developer Mode permits access to the full set of capabilities that have been built into the TrueBeam control system, not available in the clinical modes. It is driven by XML Beams loaded from local storage or network on the TrueBeam control console workstation computer. XML Beams are essentially text scripts in XML format where a rich instruction set allows Developer Mode users to construct and deliver complex non-standard beams, imaging, and gating [10]. The user interface of the developer mode does not allow modifications to any machine configuration or operational parameters which may affect the functionality of Clinical Modes.

The trajectory function, which relates the position of all mechanical axes to the Monitor Unit (MU), is described in terms of a finite number of discrete points called control points. Control Points are inflection points in the trajectory where the axis motion per MU delivered is defined. The Developer Mode is used to deliver the machine trajectory file programmed by specifying these Control Points in XML Beam file.

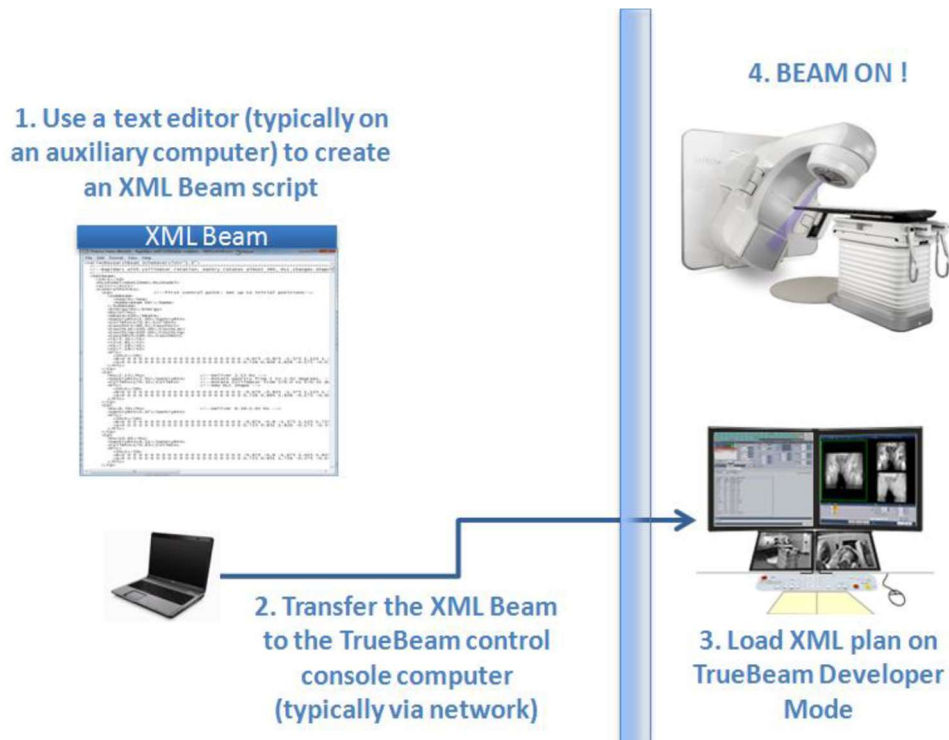


Figure 2: Workflow of developing and delivering an XML beam on TrueBeam Developer mode [10].

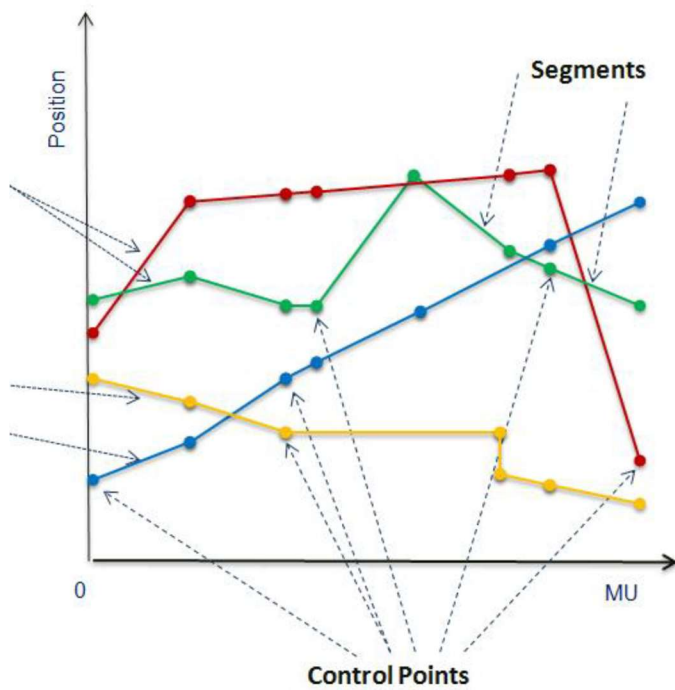


Figure 3: The trajectory function and control points [10]

1.3 Stereotactic Radiosurgery SRS and Stereotactic Body Radiation Therapy SBRT

Different external beam radiation therapy technologies were introduced, to deliver the treatment radiation dose to the tumor with a high degree of accuracy and precision. Such as the Stereotactic Radiosurgery/Stereotactic Body Therapy (SRS/SBRT), Intensity-Modulated Radiation Therapy (IMRT), Volumetric Modulated Arc Therapy (VMAT) and more [11].

SRS was introduced for the first time in the late 1940s by Leksell. He used orthovoltage x-rays to treat dysfunctional loci in the brain. Later, heavy charged particles, gamma rays, and megavoltage x-ray have been used to treat different types of brain tumors.

SRS/SBRT, is a technique for treating a lesion by means of well-collimated beams of ionizing radiation [12] [13] [14]; a high dose of single, or hypo-fractions radiation is delivered to a defined volume of tissue, the target, while the entrance and exit doses are distributed in such a way that tissue outside the target is minimally affected. This technology, in the beginning, was performed by using dedicated machines such as the Gamma Knife or Cyberknife units, however, in the last decade, all-purpose machines such as linear accelerators, tomotherapy units, or even proton therapy units have become more popular [14].

The state of the art radiotherapy techniques on a linear accelerator tend to use a number of fields with different sizes, combinations of the gantry, treatment table, and collimator rotation angles to perform the SRS/SBRT [15], and recently two additional axes of rotation, pitch and roll, were introduced to the patient support device. As a result, Stereotactic radiosurgery/Therapy has diversified from a specialty procedure performed only at comprehensive university medical centers to a widely accepted treatment regimen adopted by most radiation oncology clinics worldwide [16]. In the SRS/SBRT the outlines of the small treatment field, steep dose gradients

in the penumbra region, can be achieved either by use of drill hole collimators (cone) attached to the accelerator's gantry head or High Definition multi-leaf collimators HDMLC.

1.4 Single Isocenter-Multiple Lesion LINAC-Based SRS/SBRS

Treating planning during SRS/SBRT for the treatment of multiple lesions in LINAC-based system can be done based on one isocenter in each lesion. However, in a very recent study, researchers have shown that treating multiple lesions with one isocenter can be as accurate, efficient and requires less time to be executed [17] [18] [19] [20]. Clark et al. found in their study [17], that single-isocenter VMAT radiosurgery is extremely efficient, and requires less than one-half the beam time required for multi-isocenter for multiple targets LINAC-based treatment technique. Gao and Liu [16], found in their clinic, that the single isocenter technique can be used to treat multiple targets efficiently and accurately only when the maximum distance from the center of the mechanical field to the machine isocenter is within 3 cm. However, they emphasized that every machine has different deviation data, and every clinic needs to set investigate their machine deviation. Calvo-Ortega et al. [20] investigated the targeting accuracy of intensity-modulated SRS (IMRS) to treat multiple brain metastases with a single isocenter, they found that no statistical difference was found in the accuracy of targeting between the central and the peripheral lesions.

Huang et al. [18] compared between single-isocenter dynamic conformal arcs (SIDCA) radiosurgery and multiple-isocenter dynamic conformal arcs (MIDCA) radiosurgery to treat multiple brain metastases. They found that SIDCA has the same plan quality as MIDCA. However, more efficient than the latter. Moreover, the delivery time of SIDCA is significantly shorter than MIDCA.

In the above-mentioned studies, it is believed that single-isocenter multiple targets technique will likely replace multi-isocenter for multiple targets in LINAC-based stereotactic radiosurgery treatment technique

1.5 Quality Assurance

In general, radiation therapy is a complex process, includes multi-step procedures, starting from the beam calibration to treatment plan verification for patient treatment. Along these steps, there are measurement uncertainties and systematic or occasional deviation risks introduced. Treatment of the patient, the last step, incorporates the adding up of all these uncertainties and deviations. Hence, it is essential in radiotherapy to have quality management addressing quality procedure at each step toward the final product which is the treatment of the patient [21].

Due to the increased number of complex methods using the gantry arc to deliver the radiation to the tumor, such as SRS and SBRT; a major quality testing of the mechanical performance is required and evolved. The gantry head and its components are a multi-ton part of the LINAC, the effect of the gravity not- negligible. Therefore, the gantry is not moving in a perfectly circular track around its axis. Also, this leads to imperfect alignment in the collimation tools during the arc delivery. As a result of this eccentricity of the gantry rotation, uncertainties in field shapes are introduced and need to be addressed quantitatively and qualitatively.

The principal feature of quality assurance procedures for LINAC-based radiosurgery is verification of the mechanical tolerance, x-ray/light alignment with Isocenter and verification of the target/tumor with the Isocenter prior to treatment. The precision and the related quality assurance tests are crucial to delivering high dose to a small target. So for the SRS, the gantry

rotation axis, the table rotation axis, and the collimator rotation axis should coincide within a sphere of 1 mm radius [13] [12]. The demands on restricted quality assurance procedures for these situation results in introducing different approaches. The main approach which dominates this task is called the Winston-Lutz (WL) test [12] [14] [16] [15].

1.6 Winston-Lutz Test

In 1988, three colleagues in Harvard medical school, Wendell Lutz, Ken Winston and Nasser Maleki, introduced a new technique to test the mechanical integrity of the LINAC, represented in it the gantry, the couch, and the collimator rotation to verify its isocenter for their routinely pre-treatment QA performed for cranial stereotactic radiosurgery. Also, they wanted to verify the accuracy of patient positioning to the radiation isocenter by relying on the laser alignment. The test was given the name Winston–Lutz (WL) test. Traditional WL test localizes the isocenter of the LINAC by correlating the radiation fields directly with the object being irradiated. Usually, the irradiated object is a ball-bearing (BB) phantom with millimeters radius. The ball is aligned to the isocenter using the treatment room positioning lasers then being imaged by a circular or square collimated field, at selected gantry, collimator, couch angles. The projection of the BB should be in the center of the field in the ideal situation. The good results should show shift less than or equal to 0.5 mm. [22].

WL test checks if there is any imperfection in repositioning the cone amount system after services [22]. Performing WL test on the MLC is very important because the cone based WL test does not check the mechanical isocenter of the MLC. Also, the MLC may not be positioned correctly after service.

Another importance of WL test is the verification of the accuracy of the laser positioning system [22]; the laser system is used to position the BB in the isocenter, and if there is a significant shift in the results, the laser system accuracy must be checked.

1.7 Significance of Study and Objectives

The WL test could be performed by an experienced medical physicist in 29.0 ± 8.0 min. [23]. Running the WL test for different degrees of freedom is a time consuming; repetitive manual changing in the rotation angles of the gantry, couch, and collimator manually in each different combination is a tedious process. Also, manual mode could induce a margin of human errors, such as accidental movement of the couch between beams (from bumping or leaning on the couch), forgetting to take an image needed in the right sequence, selection of inconsistent imaging templates i.e. high resolution versus low dose imaging modes, selection of improper collimating device for test, or not choosing an all-inclusive geometry range to test all rotating axes. Automating WL Test will drastically shorten the test time. Although it is expected that the human error will be decreased, there is still a margin of human error such as poor initial positioning of the ball, no isocenter calibration performed or no MLC initialization performed.

The use of XML scripting in TrueBeam Developer Mode allows for efficient and accurate data acquisition during QA tests. The efficiency improvement is most pronounced for iterative measurements, exemplified by the time savings for imaging. The scripting also allows for the creation of the files in advance without requiring access to Treatment Planning System TPS. Finally, automation reduces the potential for human error in entering LINAC values at the machine console, and the script provides a log of measurements acquired for each session.

The automated test is designed and performed to study the single isocenter-multipole lesions conformal arc LINAC-based radiosurgery. the aperture opening from the collimating MLC with the position of the tumor at varying distances away from radiation and mechanical isocenter is investigated. In another word; to test discrepancies between the planned beam and the actual beam centers when the target interest is away from the mechanical isocenter of the machine. The purpose of this is to add more value to the QA test for utilizing LINAC in radiosurgery. Consequently, this will assist the radiation oncologist, physicist, and dosimetrist in the plan design of the better plan, and understand the delivery limitations for SRS/SBRT on LINAC machine.

CHAPTER 2:

MATERIALS AND METHOD

2.1 Experiment's Material

A Varian TrueBeam linear accelerator (Varian Medical Systems, Palo Alto, CA) was used on-site at the Varian Medical Systems Education and Training Center in Las Vegas, NV. All beams used are 6 MV photon beams. The attached electronic portal imaging device (EPID) was used to acquire the images, it was a Varian Portal Vision Digital Megavoltage Imager (DMI) EPID with aS1200 readout panel that has an active area of 43x43 cm² made up of 1280 x 1280 pixels.

The Perfect Pitch Exact couch and a ball-bearing (BB) phantom from Varian Medical Systems were utilized. The phantom consists of a steel ball (diameter: 5 mm) located at the tip of a long steel rod, which is connected to a base plate locked to the couch with a set of Vernier adjustments that allow the position of the steel ball to be adjusted in 0.01 mm increments. A cone collimator with radius 17.5 mm is attached to the head of the TrueBeam machine to collimate the beam. See figure 5.

The High Definition 120 leaves MLC (HDMLC), which comes installed inside the head of the true beam gantry, was used to collimate the 2 cm diameter beam, to study the off accesses mechanical positioning accuracy. The center of the HDMLC consists of 32 pairs of leaves, each one has 2.5 mm thickness. Where The peripheral part consists of 28 pairs of leaves, each one has 5 mm width.

2.2 EPID Quality Assurance

At the beginning of the measurement, to make sure that any discrepancy between the image center and the BB phantom center is coming only from the mechanical displacement of the LINAC gantry isocenter away from the radiation isocenter, a quality test was performed for the EPID to eliminate any possible error could result from the image acquiring. The QA test was performed by taking few MV images of the IsoCal phantom, The TrueBeam uses the IsoCal data to apply physical corrections to the panel position during image acquisition. See figure 4.

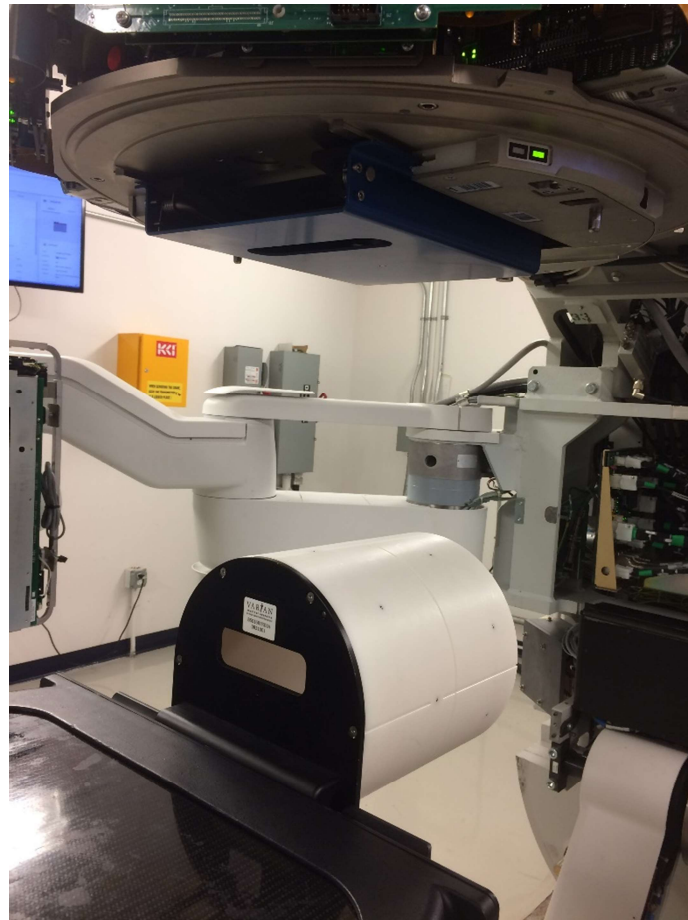


Figure 4: The IsoCal system

2.3 Automated Winston Lutz Test

The general setup of the Winston-Lutz test is illustrated in figure 5. The test was performed automatically on the TrueBeam accelerator. The first step was BB phantom is fixed to the couch by using the provided micrometer stage. The positioning laser system was used to place the BB in the isocenter of the LINAC. See figures 5 and 6.

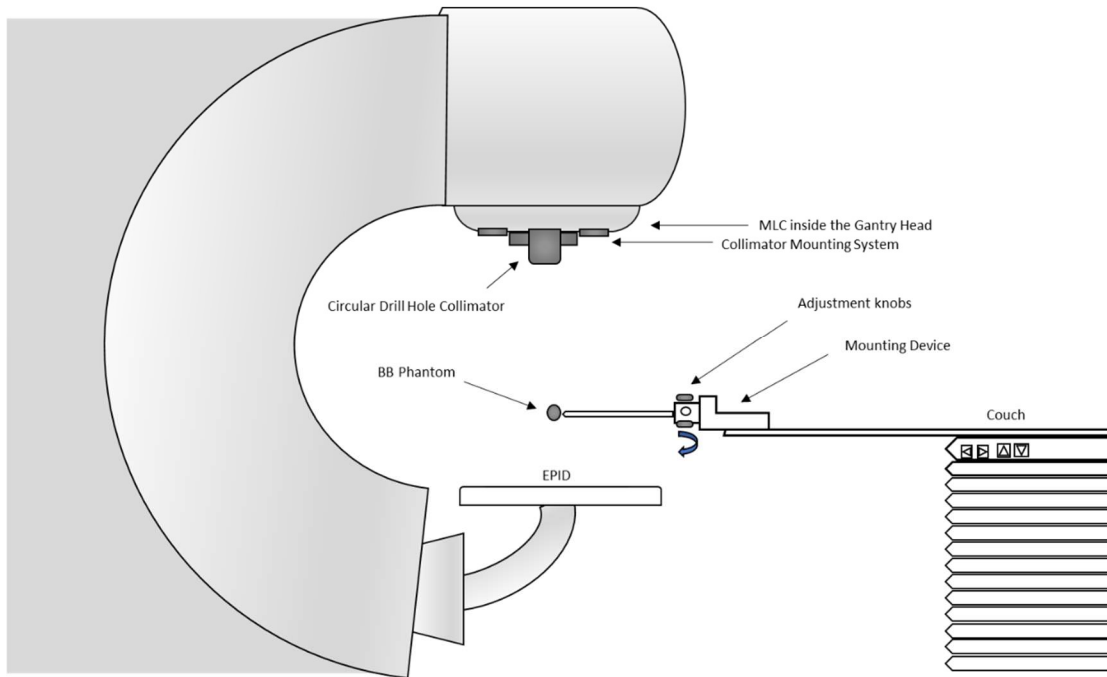


Figure 5: WL test set up on the TrueBeam LINAC using circular drill hole collimator

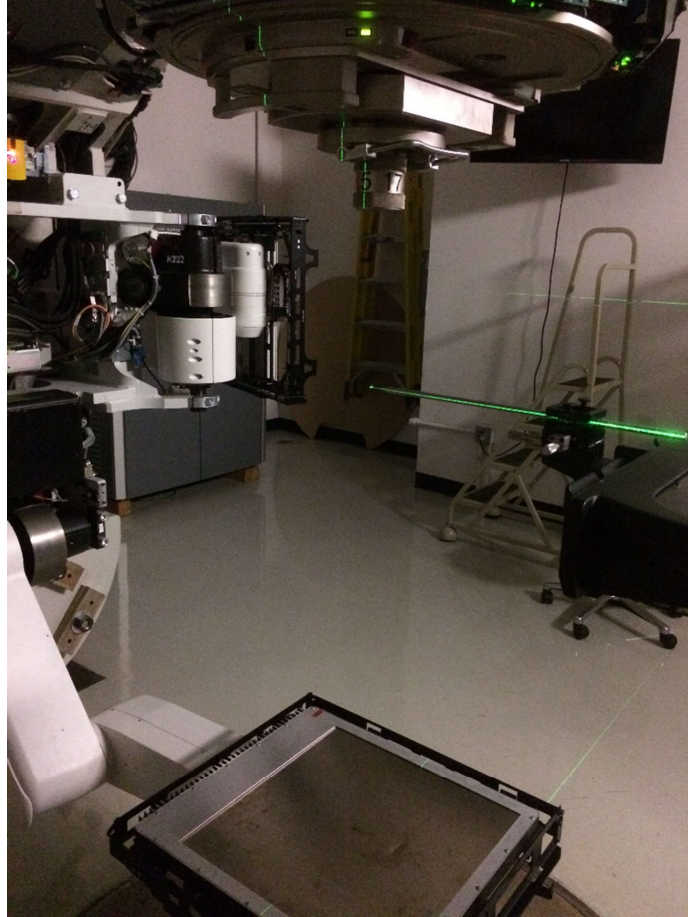


Figure 6: The BB phantom.

Beam configurations with an instantaneous image acquiring for each beam were set by writing a proper XML script and uploading it to the developer mode of the TrueBeam accelerator. There is no universal set of gantry, couch and collimator angles used in WL tests, so the set is chosen based on compromising made between obtaining sufficient samples and reducing the test time while avoiding a collision.

2.4 Automated off-Isocenter Winston-Lutz

Next step was to perform the off-isocenter Winston-Lutz. A patient has been created with multiple structure sets in the Eclipse Treatment Planning system—each structure set contains a

Planning Treatment Volume, PTV that is X cm away from isocenter of the field. The PTVs were set at distance 0, 2, 4, 6, and 8 cm diagonally superiorly to the left away from the isocenter in the superior (PA) and Then a conformal arc plan for the PTV that had been created off axis was generated. See figure 7.

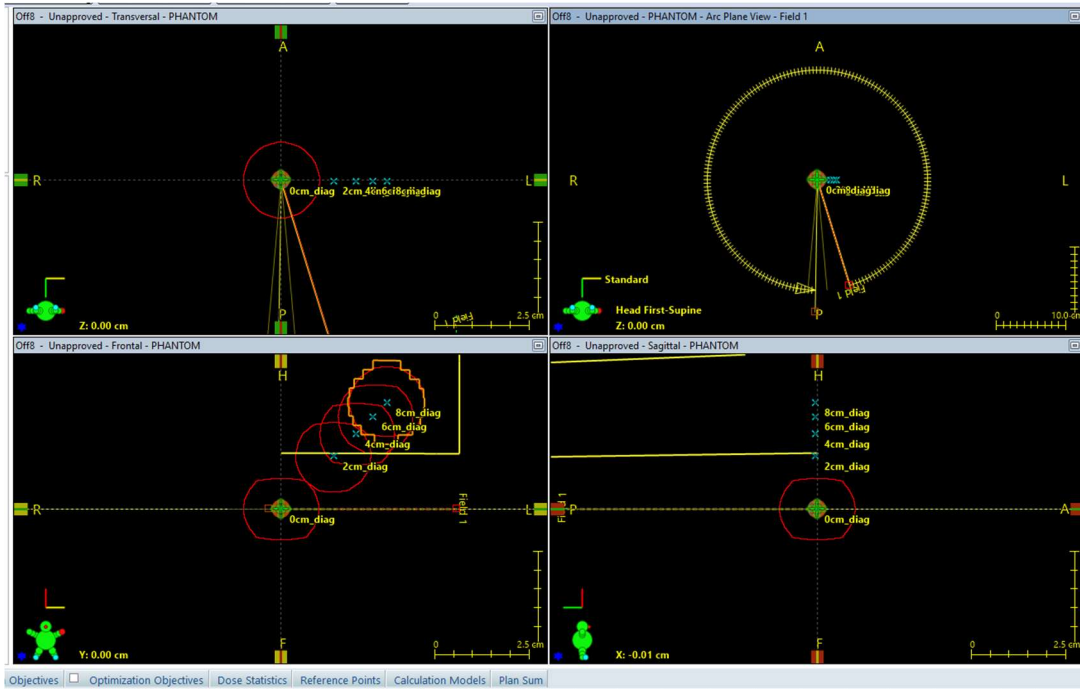


Figure 7: Eclipse conformal arc plan for different PTVs

For each PTV, the plan was exported as a DICOM file. An in-house Python code was developed to manipulate this DICOM file to use it for off-isocenter WL test. The manipulation processed was as follow: First the Python code defined and found the cardinal angles of the gantry rotation. The DICOM defines the LINAC coordinates according to the International Electrotechnical Commission (IEC) coordinate systems, however, the developer mode of the TrueBeam uses a different coordinate system, Varian coordinate. The difference between them is

illustrated in figure 8. Therefore, the python code converts the coordinate system from Varian to standard scale.

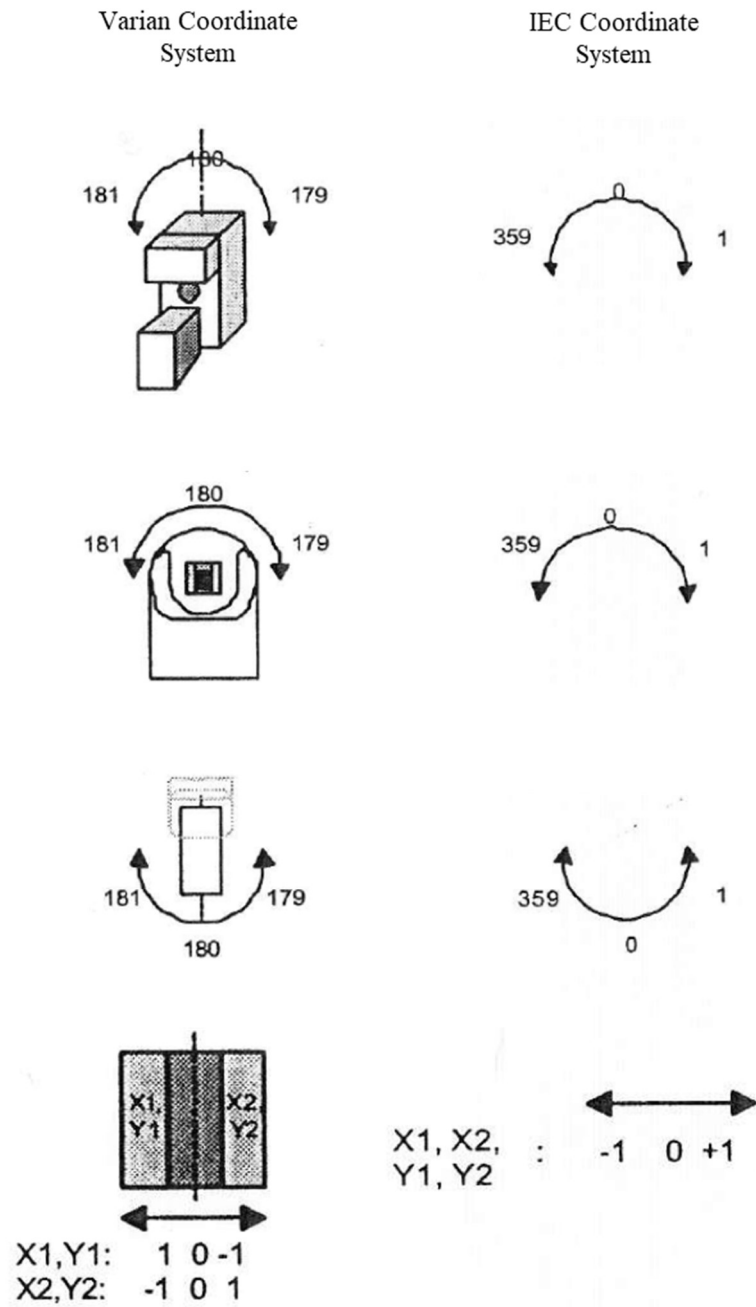


Figure 8: The differences between Varian and the standard system.

Second, the code would find the control points at each cardinal angle. The code would interpolate the control points to get the index of the control point at a particular cardinal angle. Third, the code would find the MLC positions for each control point at the cardinal angles. Also, the code would interpolate the leaf positions accordingly with the interpolated control points index. Finally, the code would build XML script and save it as an XML file. This script is ready to be fed to the developer mode of the TrueBeam to run it directly without any changes; it would rotate the gantry to the cardinal angle, adjust the MLC leaves into their particular positions and take images of the BB phantom and save these images. The BB was centered in the light field rather than the laser pointers to make sure it is precisely in the middle of the beam. This was done vertically and laterally, see figure 9. The summary of the workflow is presented in figure 10.

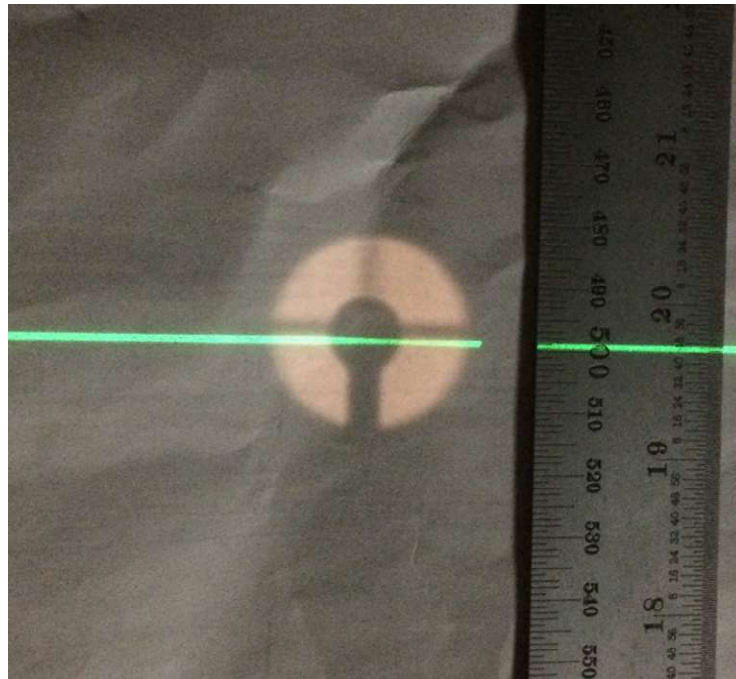


Figure 9: Centering the BB phantom in the light field

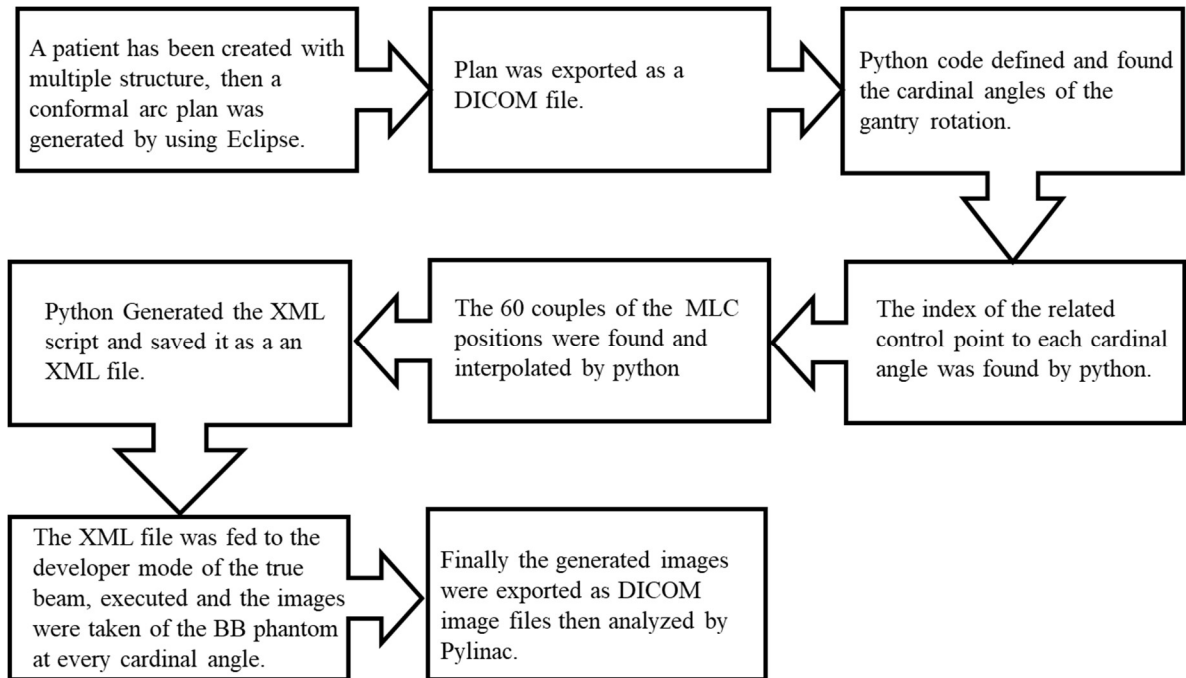


Figure 10: The workflow of the off-isocenter WL test

The LINAC couch has elasticity some which will result in a very limited binding when the patient lies down on it for treatment. This small binding will generate a significant deviation in beam targeting precision, especially in SRS/SBRT. It was measured that a pitch angle of 1.5 degrees corresponded to a shift in the translational direction of 3 to 4 mm. for a 3 degrees pitch shift, the translational shift would be from 6 to 7 mm [24]. Because of this unwanted shift, Varian came up with the robotic 6DoF couch, which can compensate the pitch angle up to 3-degree angle, and it can hold up to 200 kg weight. see figure 11. To mimic the clinical practice in this study, phantom and solid water, of total around 75 kg, were applied on the couch to perform the off-isocenter study, see figure 12, then the images of the BB phantom where taken at the cardinal angles for different off-isocenter distances number of times. Later, the weight was removed and the same processes were repeated.

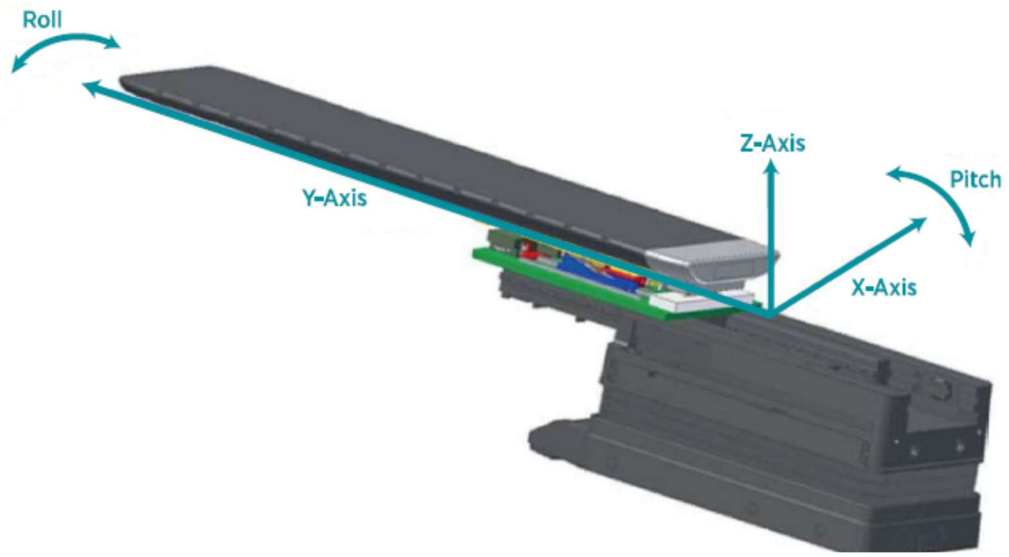


Figure 11: The robotic 6DoF couch.



Figure 12: The weight-loaded couch to mimic the clinical situation

2.5 Analyzing the Images

The manual analysis can be performed by using the EPID based software built into the True Beam's XI tab of Service Mode, the measurements are taken visually to check the difference between radiation isocenter and the image centers. However, this method is time-consuming and there is a risk of personal errors in taking the variation visually then calculating the variation, especially if there is a large number of images need to be analyzed per one WL test.

Consequently, there are several available software packages that can assist with WL test image analysis, most of them are in-house developed software [16] [9] [8] [23], some of them are populated to be used by any interested person for free. Also, there are some commercial packages can be utilized for the same purpose. This software automatically takes the DICOM images file and generate a detailed report about the shifts and errors in the taken images of the WL test.

In this work, Pylinac Full Scale Analysis Package was used. It provides QA tools to Python programmers for the American Association of Physicists in Medicine (AAPM) Task Group 142 (TG-142) [25]. It contains different modules, and WL module is one of them, which is used in this work. WL module algorithm automatically finds the Central AXial (CAX), which is a line perpendicular to the cross-section of treatment field, and the BB, along with the vector and scalar distance between them. It also finds the 3D gantry isocenter size and position and the 2D planar isocenter size of the collimator by using back projections of the EPID images. In the end, WL module plots the variation of the gantry as well as Root Mean Square (RMS) variation.

Pylinac is using different coordinate system than Varian or IEC coordinate system as in figure 13, the positive x-direction is to the right of the couch, the positive y-direction is upward, and the positive z-direction is toward the gantry.

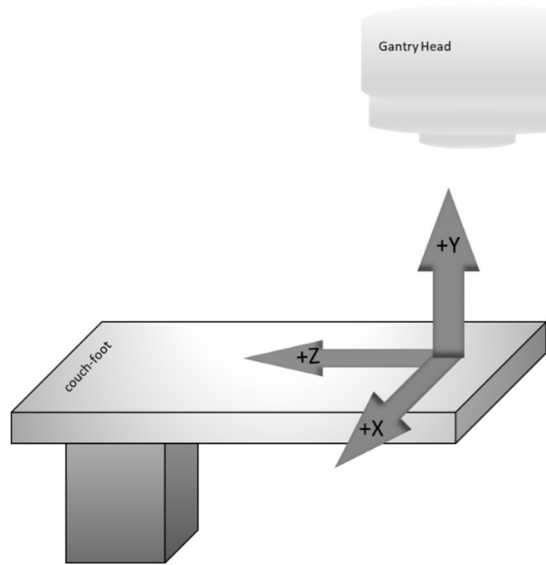


Figure 13: The coordinate system used in Pylinac

CHAPTER 3:

RESULTS

The XML script for the automated Winston Lutz was compiled and executed successfully, figure 14 shows the different combination of gantry rotation and couch rotation angles. The total 20 images were acquired, and the total time since starting the first beam until the gantry went back to its vertical position was 12:57 minutes. The images were taken in couples, each couple has opposite gantry angle to create CAX. Appendix 1, shows the XML code. It can be populated to be used by any medical physicist for his/her clinical practice. Also, the code can easily be edited to perform a different number of images or adding/removing a specific degree of freedom.

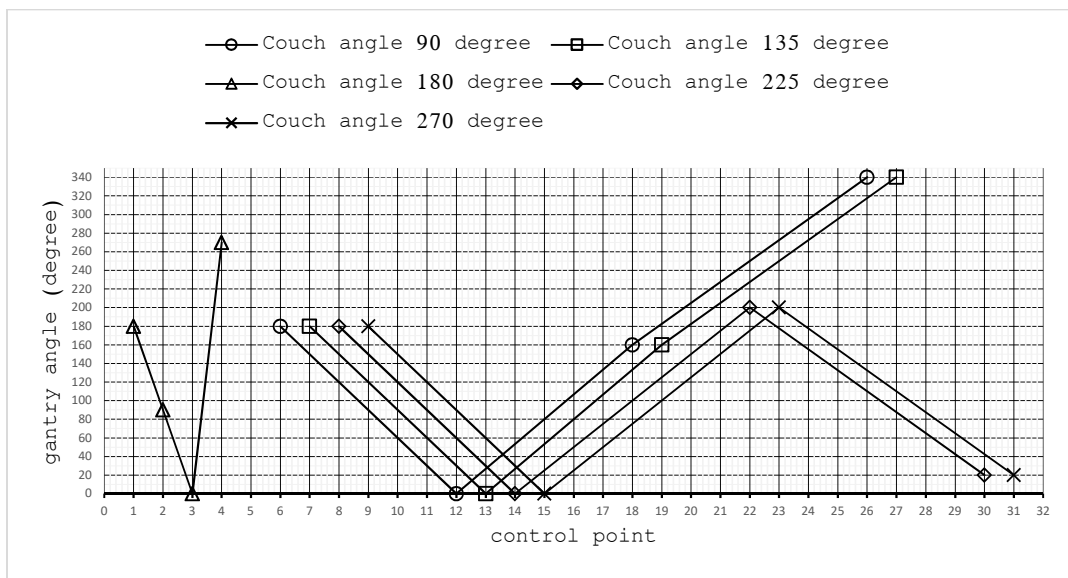


Figure 14: The couch and gantry angle configuration versus the control points for the 20 images WL test

Figure 15 shows an example how the report would be generated by Pylinac after analyzing the image. In this selected part of the results report, it presents the mean and the maximum x, y and z components of the displacement vector from the gantry isocenter of the

used LINAC to the center of the BB phantom. Also, it graphs the 2 dimensions (2D) shifts between the CAX and the center of the BB phantom at every cardinal angle. There is a part of the report where it presents the images with indicating the amount of shift in each one of them.

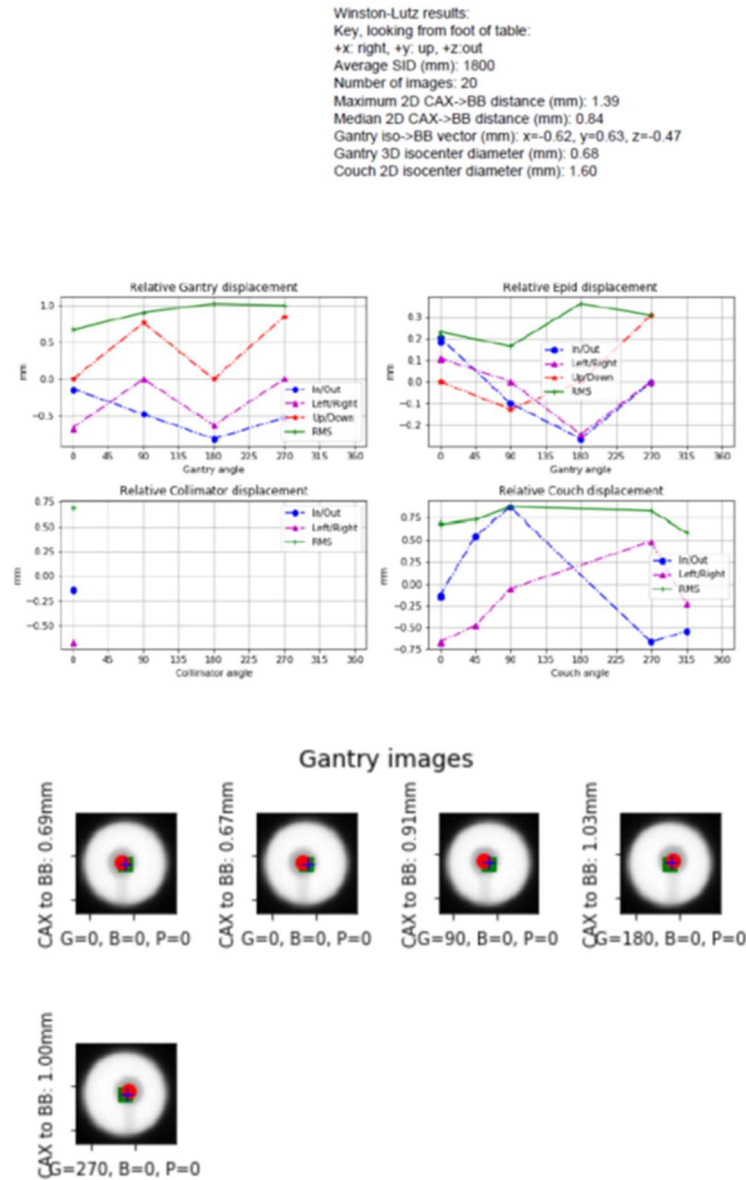


Figure 15: An example of selected part of the results report generated by Pylinac [25].

The in-house python code was compiled and run successfully to generate the XML script, which is needed to perform the off-isocenter Winston Lutz test, see appendix 2. The following results are for the deviation when the weight was loaded on the couch, unless no weight on the couch was mentioned.

For each off-isocenter distance, five measurements were taken for the reproducibility. the mean x, y and z components displacement vector from the gantry isocenter of the used LINAC and the center of the BB phantom are presented in table1. Figure 16 is the plot of the mean deviations from the first three columns in table1, and the maximum deviations are plotted in figure 17.

Table 1: The x, y and z-direction of the maximum shift of the BB from the isocenter

off-isocenter shift (cm)	Δx (mm)	Δy (mm)	Δz (mm)
0.0	-0.10	0.00	-0.18
2.0	0.29	0.09	-0.42
4.0	-0.02	0.71	-0.22
6.0	-0.48	0.71	-0.76
8.0	0.24	0.48	-0.24

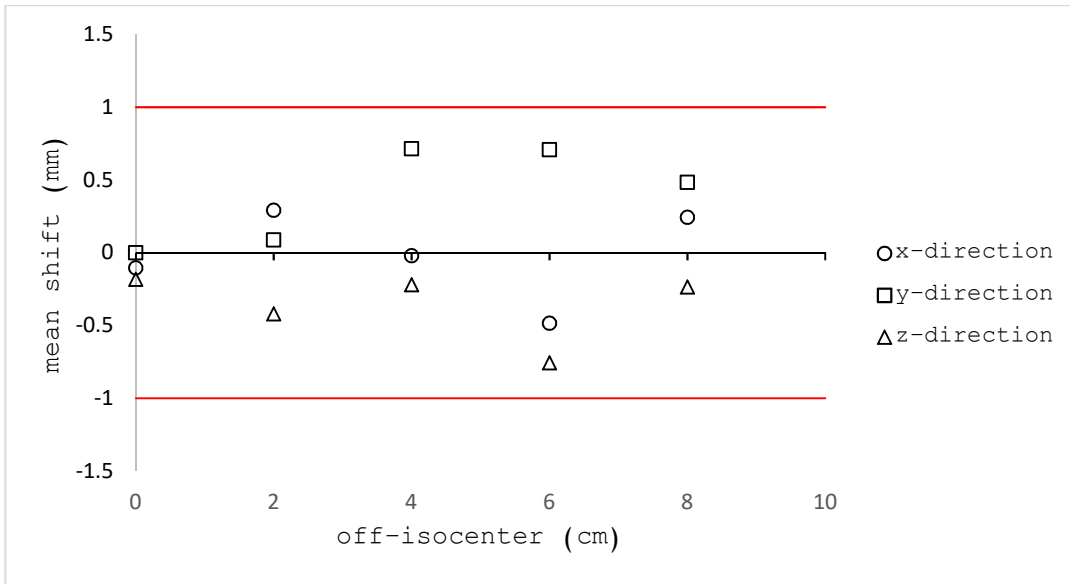


Figure 16: The x, y and z-direction of the maximum shift of the BB from the isocenter

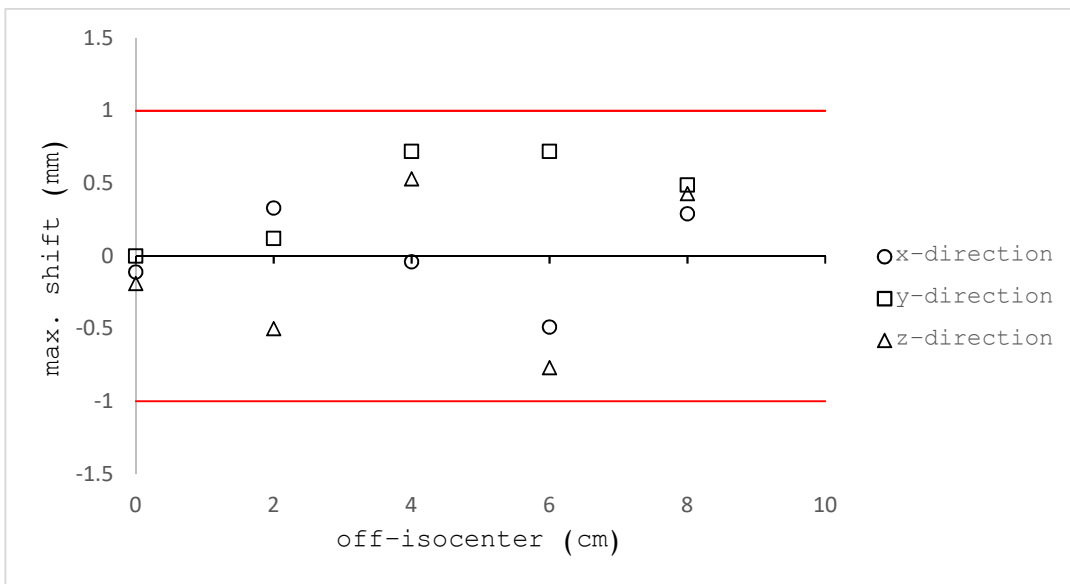


Figure 17: The x, y and z-direction of the maximum shift of the BB from the isocenter

The results from Pylinac also show the maximum 2D shift between the center of the BB phantom and the CAX. The results are presented in table 2, and the maximum and the minimum deviations are plotted in figure 18. As it can be seen, at 4 cm off-distance center, the maximum

shift larger than 1 mm by 3%. however, at 6 cm off-isocenter, the maximum and medium shifts are 14% and 8% higher respectively.

Table 2: The maximum and median 2D shifts between the CAX and the BB, for different off-isocenter displacement.

off-isocenter shift (cm)	Max 2D CAX->BB distance (mm)	median 2D CAX->BB distance (mm)
0.0	0.48	0.31
2.0	0.81	0.71
4.0	1.03	0.53
6.0	1.14	1.08
8.0	0.834	0.72

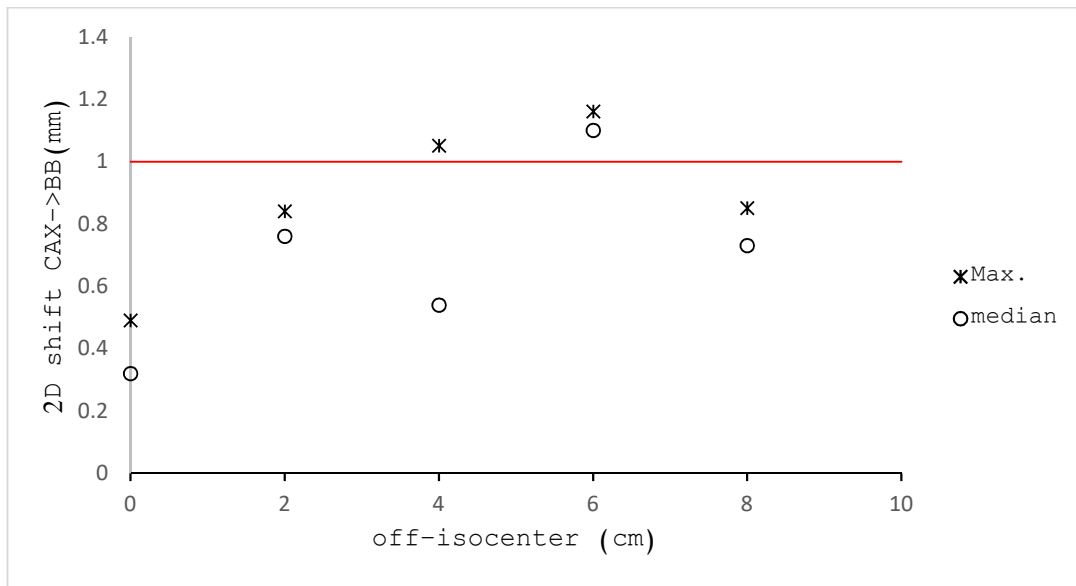


Figure 18: The maximum and median 2D shifts between the CAX and the BB, for different off-isocenter displacement.

To investigate the 2D shifts in the BB position more, they were obtained at every gantry angle, table 3 shows their values, where they were plotted in figure 19. It can be shown, that the shifts are higher, when the BB was off-isocenter, at gantry angle 90 and 270 degrees. When the

BB was 6 cm, the shifts in position was more than 1 mm between 8% and 14%. Also, it can be noticed that there is no clear correlation between the BB shifts and its off-isocenter displacement.

Table 3: The maximum 2D shifts between the CAX and the BB, for different off-isocenter displacement

gantry angle (degree)	CAX to BB (mm)				
	0 off-axis	2cm off-axis	4cm off-axis	6cm off-axis	8cm off-axis
0.00	0.30	0.21	0.53	1.12	0.45
90.00	0.16	0.53	1.03	1.14	0.83
180.00	0.23	0.37	0.78	1.13	0.64
270.00	0.29	0.71	0.90	1.08	0.61
Avg	0.25	0.45	0.81	1.12	0.63
max	0.30	0.71	1.03	1.14	0.83

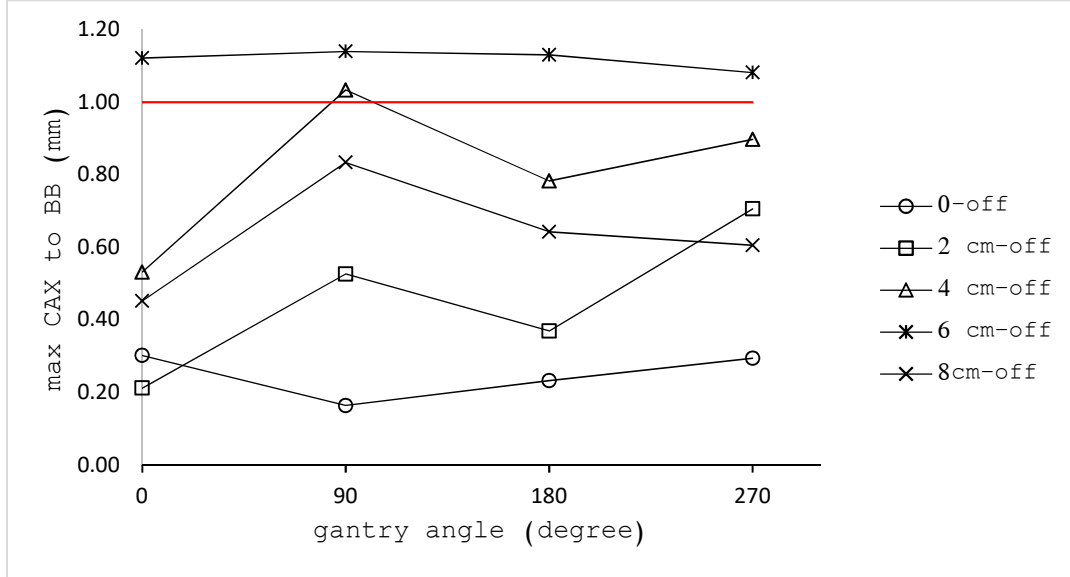


Figure 19: The maximum 2D shifts between the CAX and the BB, for different off-isocenter displacements, versus the gantry angle.

When the couch was load free, the x, y and z components of the displacement vector from the gantry isocenter to the center of the BB phantom, for different off-isocenter distances, were measured, then compared to their mean value when the weight was loaded on the couch. The difference between them is shown in figure 20.

It can be seen from figure 21, that the shift in the y-direction, which is in the vertical direction, is huge comparing to the x and z directions. This result was expected because of the weight compensation with the pitch and roll degree of freedom.

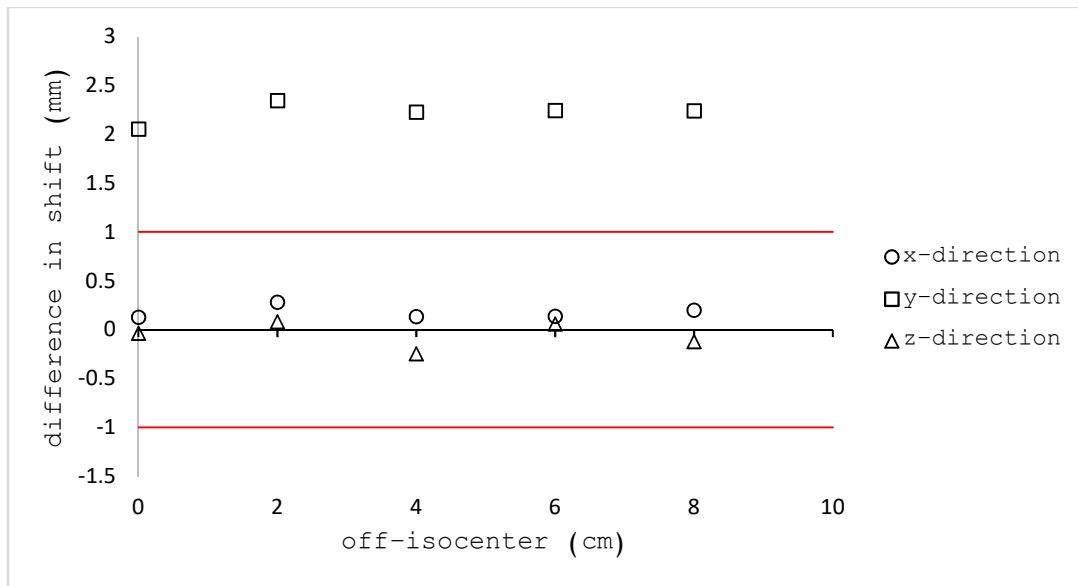


Figure 20: The difference in the x, y and z-direction of the shift of the BB from the isocenter between the loaded and unloaded couch.

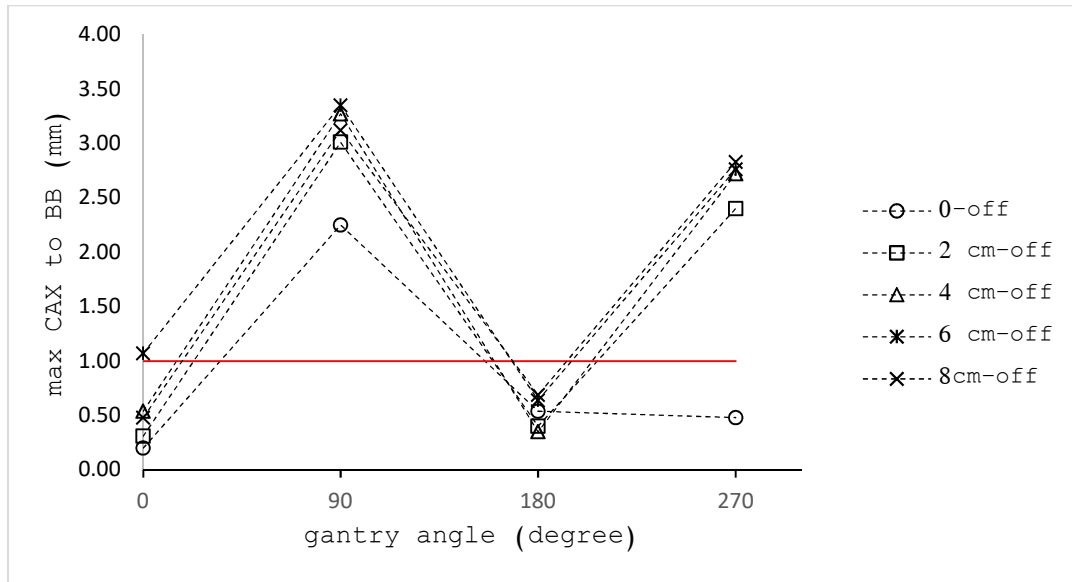


Figure 21: The maximum shift of the BB from the CAX versus the gantry angle, when the couch is unloaded

CHAPTER 4:

DISCUSSION

The automated WL test was executable; the total time for 20 images was 12:57 minutes comparing to 29 min for simple manual WL images. The time even could be shorter if less number of images were acquired, this depends on the clinical practice for every physicist who is performing the QA test on LINAC. The XML script can be modified easily to achieve the desired number of images or even to modify any of the coordinate. During the test there was no need to go inside the treatment room to change any degree of freedom between the images, this is shortening the procedure time and minimizing the chance of errors to occur.

The compiled Python code was effectively able to extract, from the exported DICOM conformal arc plan file, the cardinal angles and the corresponding leaves coordinate at each one. Also, the Python code was effective to generate the XML script for the off-isocenter WL test. The resultant XML script was utilized in the developer mode of the TrueBeam without errors. The Pylinac code analyzed the images of WL test effectively and quick. Then the whole process, starting from DICOM file of the treatment plan to the final results of the analyzed images was successful and doable.

The mechanical motion cannot be absolutely accurate in the real world, when the gantry rotates to a specific angle, there always uncertainty present. The wobbling of the radiation field around the radiation isocenter mainly comes from the non-ideal gantry rotation because of the

gravity of several tons of radiation generating and shielding materials inside the gantry, which causes the gantry rotation to deviate from the ideal trajectory; a perfect circle about the rotation axis. The recommended maximum allowed uncertainty in gantry position and couch positioning, according to TG-142, is 1.0 mm. The results of the off-isocenter WL test, for all the off-isocenter displacements, except the 6 cm displacement, showing that all the three components of the displacement vector between the beam isocenter and the center of the BB is within that range of tolerance. Regarding the aberration of the measurement at 6 cm off-isocenter, another 5 measurements were taken for consistency, and yet the result was consistent with the result of the first 5 measurements. The possibility of error in the treatment planning was eliminated since the same one was used for all the off-isocenters distances. However, after a fine inspection of the treatment planning simulation, there was a significant shift between the center of the PTV and the reference point, although the reference point was set on the center of the PTV in the plan. As in figure 22, the blue cross represents the reference point and the cross dashed lines represent the center of the PTV. The reasonable explanation of this eccentricity is as follow: The virtual CT image that was used in Eclipse TPS has a slice interval of 0.25 cm. When the PTV was displaced diagonally 6 cm from the isocenter, that means a displacement of 2.45 cm was placed in each direction; linguodental and lateral. Since Eclipse defines the 3D contour from each 2D planar contour, contours have to live on the CT slices, whereas the edges of the 1 cm radius PTV were not, because the distal and the proximal edges were at 1.45 cm and 3.45 cm respectively, and neither the of the positions live on a slice interval. In order for the Eclipse to keep the structure as a sphere as it was asked, it is possible that it shifted the PTV onto a slice (say for example to 3.5cm and 1.5cm in order to keep it the same diameter, which pushed it 0.5mm away from the

reference point. This action does not falsify the dose calculation in Eclipse since it can interpolate between slices to tell you what the dose would be at the reference point.

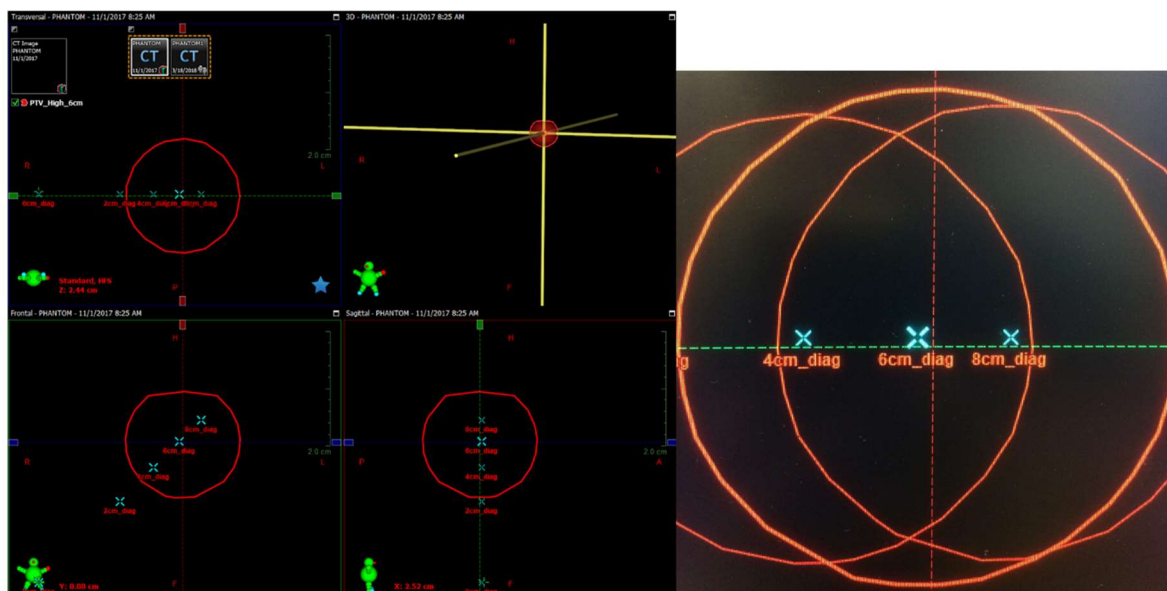


Figure 22: on the left, the transverse, frontal and sagittal views of the PTV. On the right, zoomed view of the transverse view showing the shift between the reference point and the center of the PTV.

The perfect pitch and roll 6DoF robotic couch are very important for the accuracy of the SRS/SBRT techniques, according to the results in figures 20 and 21, the couch adjusted itself in the x, y, and z-direction to compensate for the loaded weight. The most pronounced adjustment was in the vertical direction (y-direction). The maximum and the mean adjustment were 2.3 mm and 2.2 mm respectively. These shifts would be an added inaccuracy to the positioning of the target if the couch had not adjusted itself.

CHAPTER 5:

CONCLUSION & RECOMMENDATIONS

LINAC-based SRS/SBRT is well practice modality to treat small tumors, however, it needs a restricted QA test for the spatial accuracy of targeting. WL test is an effective and reliable mechanism to perform the QA for this purpose. Automating WL test shortened the running time, and needs one time setting of the WL test kit. This also decreases the chances of human errors and hustle.

The results of this work, which was done for incremental off-isocenter displacements up to 8 cm, indicates that the single isocenter conformal arc SRS/SPRT can produce high conformal radiosurgery, regarding the spatial accuracy. The results of off-isocenter WL test shows a spatial inaccuracy, yet it still within the allowed tolerance according to TG-142 and TG-101 report. that single-isocenter multiple targets technique will likely replace multi-isocenter for multiple targets in LINAC-based stereotactic radiosurgery treatment technique.

The perfect pitch and roll 6DoF played a very important role in adjusting the target spatial position in the center of the treatment beam. This adjustment can make a big difference in covering the PTV and avoiding Organ At Risk (OAR). In the cases of SRS/SBRT, this 6DoF couch is essential.

It is recommended to adopt the automated WL to verify the isocenter of the gantry, couch and collimator rotation for routinely pre-treatment QA. Also, it is recommended to use the

automated WL to check if there is any imperfection in repositioning the cone amount system after services as well as to check the perfect reposition of MLC after service. The accuracy of the laser positioning system could also be tested by automated WL test.

Depending on the clinical practice for every QA tester, it is recommended that the medical physicist who is in charged with the periodic QA test for the LINAC-based SRS/SBRT, to change the XML code to give the optimum results that he or she is looking for. It needs a minimum knowledge of the XML scripting. The test could be done in the routine QA test and before each procedure.

The WL off-isocenter study needs to be performed on higher level of capabilities and more resources to verify and count on its results, to establish a guideline for the single isocenter-multiple lesion radiosurgery, which can be likely included as a supplement to the current standard QA procedure in future updates of the AAPM TG-142 and TG-101 reports, as well as the ASTRO SRS/SBRT, reports. The study needs to be performed on different LINAC machines and more measurements by different testers. This would support the confidence of the results since it provides more reproducibility, repeatability, and more statistical analysis to support any role could be stated at the end.

APPENDICES

Appendix 1: The XML script for 20 images WL test

```
<VarianResearchBeam SchemaVersion="1.0">
  <!--*****-->
  <!--20 -->
  <!--*****-->
  <SetBeam>
    <Id>1234</Id>
    <MLCModel>NDS120HD</MLCModel>
    <Accs>
      <Acc2>3317</Acc2>
    </Accs>
    <ControlPoints>
      <Cp> <!--control point 0 (zero).-->
        <SubBeam>
          <Seq>0</Seq>
          <Name>MV Outside</Name>
        </SubBeam>
        <Energy>6x</Energy>
        <Mu>0</Mu>
        <DRate>400</DRate>
        <GantryRtn>180.00</GantryRtn>
        <CollRtn>180.0</CollRtn>
        <CouchRtn>180</CouchRtn>
        <Y1>2.5</Y1>
        <Y2>2.5</Y2>
        <X1>2.5</X1>
        <X2>2.5</X2>
      </Cp>
      <!--4 gantry angle (270,0,180,90) with couch at 180.-->
      <Cp> <!--control point 1 .-->
      </Cp>
      <Cp> <!--control point 2 .-->
        <GantryRtn>90.00</GantryRtn>
      </Cp>
      <Cp> <!--control point 3 .-->
        <GantryRtn>0.00</GantryRtn>
      </Cp>
      <Cp> <!--control point 4 .-->
        <GantryRtn>270.00</GantryRtn>
      </Cp>
      <!--2 gantry angle (180 and 0/360 (depends on couch angle))
with couch at 90, 135, 225, and 270.-->
      <!--gantry 180-->
      <Cp> <!--control point 5 .-->
        <GantryRtn>180.00</GantryRtn>
      </Cp>
      <Cp> <!--control point 6 .-->
        <CouchRtn>90</CouchRtn>
      </Cp>
      <Cp> <!--control point 7 .-->
        <CouchRtn>135</CouchRtn>
      </Cp>
      <Cp> <!--control point 8 .-->
        <CouchRtn>225</CouchRtn>
```



```

</Cp>
<Cp> <!--control point 9 .-->
      <CouchRtn>270</CouchRtn>
</Cp>
<!-- Gantry rotate to zero, couch still 225.-->
<Cp> <!--control point 10 .-->
      <CouchRtn>180</CouchRtn>
</Cp>
<!-- Gantry rotate to zero.-->
<Cp> <!--control point 11 .-->
      <GantryRtn>0.00</GantryRtn>
</Cp>
<Cp> <!--control point 12 .-->
      <CouchRtn>90</CouchRtn>
</Cp>
<Cp> <!--control point 13 .-->
      <CouchRtn>135</CouchRtn>
</Cp>
<Cp> <!--control point 14 .-->
      <CouchRtn>225</CouchRtn>
</Cp>
<Cp> <!--control point 15 .-->
      <CouchRtn>270</CouchRtn>
</Cp>
<!--2 gantry angle (200/160 and 20/340 (again depends on
couch angle) with couch at 90,135,225, and 270.-->
<!--rotate couch first 180-->
<Cp> <!--control point 16 .-->
      <CouchRtn>180</CouchRtn>
</Cp>
<!-- Gantry rotate to 160.-->
<Cp> <!--control point 17 .-->
      <GantryRtn>160.00</GantryRtn>
</Cp>
<Cp> <!--control point 18 .-->
      <CouchRtn>90</CouchRtn>
</Cp>
<Cp><!--Control Point 19-->
      <CouchRtn>135</CouchRtn>
</Cp>
<Cp><!--Control Point 20-->
      <CouchRtn>180</CouchRtn>
</Cp>
<Cp> <!--control point 21 .-->
      <GantryRtn>200</GantryRtn>
</Cp>
<Cp> <!--control point 22 .-->
      <CouchRtn>225</CouchRtn>
</Cp>
<Cp> <!--control point 23 .-->
      <CouchRtn>270</CouchRtn>
</Cp>
<!--rotate couch first 180-->
<Cp> <!--control point 24 .-->
      <CouchRtn>180</CouchRtn>
</Cp>
<!-- Gantry rotate to 20.-->
<Cp> <!--control point 25 .-->
      <GantryRtn>340.00</GantryRtn>
</Cp>
<Cp> <!--control point 26 .-->
      <CouchRtn>90</CouchRtn>
</Cp>

```

```

    <Cp> <!--control point 27 .-->
        <CouchRtn>135</CouchRtn>
    </Cp>
    <Cp><!-- Control Point 28-->
        <CouchRtn>180</CouchRtn>
    </Cp>
    <Cp><!-- Control Point 29-->
        <GantryRtn>20</GantryRtn>
    </Cp>
    <Cp> <!--control point 30 .-->
        <CouchRtn>225</CouchRtn>
    </Cp>
    <Cp> <!--control point 31 .-->
        <CouchRtn>270</CouchRtn>
    </Cp>
    <!--RESET.-->
    <Cp> <!--control point 32 .-->
        <CouchRtn>180</CouchRtn>
    </Cp>
    <Cp> <!--control point 33 .-->
        <GantryRtn>180.00</GantryRtn>
    </Cp>
</ControlPoints>
<!--
*****
    Here is where we specify that outside treatment mode
*****-->
    <ImagingParameters>
        <OutsideTreatment>
            <MaxMu>100</MaxMu> <!-- This is just a limit of max
MU to be delivered. Actual MU delivered will be just what is enough to take the MV
image we are requesting.-->
        </OutsideTreatment>
    </ImagingParameters>
    <!--
*****
    Here is where we specify the Imaging Points
*****-->
    <ImagingPoints>
        <ImagingPoint>
            <Cp>0</Cp>
            <Acquisition>
                <AcquisitionId>0</AcquisitionId>
                <AcquisitionSpecs />
                <AcquisitionParameters>
                    <ImageMode id="Highres" />
            </Acquisition>
            <CalibrationSet>DefaultCalibrationSetId</CalibrationSet>
                <MV />
            </CalibrationSet>
            <AcquisitionParameters>
                </AcquisitionParameters>
            </AcquisitionParameters>
            <Mvd>
                <Positions>
                    <Lat>0</Lat><Lng>0</Lng><Vrt>-80</Vrt><Pitch>0</Pitch>
                </Positions>
            </Mvd>
        </ImagingPoint>
        <ImagingPoint>
            <Cp>1</Cp>
            <Acquisition>
                <AcquisitionId>1</AcquisitionId>
                <AcquisitionSpecs />
                <AcquisitionParameters>

```

```

<ImageMode id="Highres" />

<CalibrationSet>DefaultCalibrationSetId</CalibrationSet>
    <MV />
    </AcquisitionParameters>
</Acquisition>
<Mvd>
    <Positions>

<Lat>0</Lat><Lng>0</Lng><Vrt>-80</Vrt><Pitch>0</Pitch>
    </Positions>
    </Mvd>
</ImagingPoint>
<ImagingPoint>
    <Cp>2</Cp>
    <Acquisition>
        <AcquisitionId>2</AcquisitionId>
        <AcquisitionSpecs />
        <AcquisitionParameters>
            <ImageMode id="Highres" />

<CalibrationSet>DefaultCalibrationSetId</CalibrationSet>
    <MV />
    </AcquisitionParameters>
</Acquisition>
<Mvd>
    <Positions>

<Lat>0</Lat><Lng>0</Lng><Vrt>-80</Vrt><Pitch>0</Pitch>
    </Positions>
    </Mvd>
</ImagingPoint>
<ImagingPoint>
    <Cp>3</Cp>
    <Acquisition>
        <AcquisitionId>3</AcquisitionId>
        <AcquisitionSpecs />
        <AcquisitionParameters>
            <ImageMode id="Highres" />

<CalibrationSet>DefaultCalibrationSetId</CalibrationSet>
    <MV />
    </AcquisitionParameters>
</Acquisition>
<Mvd>
    <Positions>

<Lat>0</Lat><Lng>0</Lng><Vrt>-80</Vrt><Pitch>0</Pitch>
    </Positions>
    </Mvd>
</ImagingPoint>
<ImagingPoint>
    <Cp>4</Cp>
    <Acquisition>
        <AcquisitionId>4</AcquisitionId>
        <AcquisitionSpecs />
        <AcquisitionParameters>
            <ImageMode id="Highres" />

<CalibrationSet>DefaultCalibrationSetId</CalibrationSet>
    <MV />
    </AcquisitionParameters>
</Acquisition>

```

```

        <Mvd>
            <Positions>
<Lat>0</Lat><Lng>0</Lng><Vrt>-80</Vrt><Pitch>0</Pitch>
                </Positions>
            </Mvd>
        </ImagingPoint>
    <ImagingPoint>
        <Cp>6</Cp>
        <Acquisition>
            <AcquisitionId>5</AcquisitionId>
            <AcquisitionSpecs />
            <AcquisitionParameters>
                <ImageMode id="Highres" />
        </Acquisition>
    </ImagingPoint>
<CalibrationSet>DefaultCalibrationSetId</CalibrationSet>
    <MV />
    </AcquisitionParameters>
</Acquisition>
<Mvd>
    <Positions>
<Lat>0</Lat><Lng>0</Lng><Vrt>-80</Vrt><Pitch>0</Pitch>
        </Positions>
    </Mvd>
</ImagingPoint>
<ImagingPoint>
    <Cp>7</Cp>
    <Acquisition>
        <AcquisitionId>6</AcquisitionId>
        <AcquisitionSpecs />
        <AcquisitionParameters>
            <ImageMode id="Highres" />
    </Acquisition>
</ImagingPoint>
<CalibrationSet>DefaultCalibrationSetId</CalibrationSet>
    <MV />
    </AcquisitionParameters>
</Acquisition>
<Mvd>
    <Positions>
<Lat>0</Lat><Lng>0</Lng><Vrt>-80</Vrt><Pitch>0</Pitch>
        </Positions>
    </Mvd>
</ImagingPoint>
<ImagingPoint>
    <Cp>8</Cp>
    <Acquisition>
        <AcquisitionId>7</AcquisitionId>
        <AcquisitionSpecs />
        <AcquisitionParameters>
            <ImageMode id="Highres" />
    </Acquisition>
</ImagingPoint>
<CalibrationSet>DefaultCalibrationSetId</CalibrationSet>
    <MV />
    </AcquisitionParameters>
</Acquisition>
<Mvd>
    <Positions>
<Lat>0</Lat><Lng>0</Lng><Vrt>-80</Vrt><Pitch>0</Pitch>
        </Positions>
    </Mvd>

```

```

        </ImagingPoint>
        <ImagingPoint>
            <Cp>9</Cp>
            <Acquisition>
                <AcquisitionId>8</AcquisitionId>
                <AcquisitionSpecs />
                <AcquisitionParameters>
                    <ImageMode id="Highres" />
            </Acquisition>
        </ImagingPoint>
    </ImagingPoint>
    <CalibrationSet>DefaultCalibrationSetId</CalibrationSet>
        <MV />
    </AcquisitionParameters>
</Acquisition>
<Mvd>
    <Positions>
        <Lat>0</Lat><Lng>0</Lng><Vrt>-80</Vrt><Pitch>0</Pitch>
    </Positions>
</Mvd>
</ImagingPoint>
<ImagingPoint>
    <Cp>12</Cp>
    <Acquisition>
        <AcquisitionId>9</AcquisitionId>
        <AcquisitionSpecs />
        <AcquisitionParameters>
            <ImageMode id="Highres" />
    </Acquisition>
</ImagingPoint>
<CalibrationSet>DefaultCalibrationSetId</CalibrationSet>
    <MV />
</AcquisitionParameters>
</Acquisition>
<Mvd>
    <Positions>
        <Lat>0</Lat><Lng>0</Lng><Vrt>-80</Vrt><Pitch>0</Pitch>
    </Positions>
</Mvd>
</ImagingPoint><ImagingPoint>
    <Cp>13</Cp>
    <Acquisition>
        <AcquisitionId>10</AcquisitionId>
        <AcquisitionSpecs />
        <AcquisitionParameters>
            <ImageMode id="Highres" />
    </Acquisition>
</ImagingPoint>
<CalibrationSet>DefaultCalibrationSetId</CalibrationSet>
    <MV />
</AcquisitionParameters>
</Acquisition>
<Mvd>
    <Positions>
        <Lat>0</Lat><Lng>0</Lng><Vrt>-80</Vrt><Pitch>0</Pitch>
    </Positions>
</Mvd>
</ImagingPoint>
<ImagingPoint>
    <Cp>14</Cp>
    <Acquisition>
        <AcquisitionId>11</AcquisitionId>
        <AcquisitionSpecs />
        <AcquisitionParameters>
    </AcquisitionParameters>
    </Acquisition>
</ImagingPoint>

```

```

<ImageMode id="Highres" />

<CalibrationSet>DefaultCalibrationSetId</CalibrationSet>
    <MV />
    </AcquisitionParameters>
</Acquisition>
<Mvd>
    <Positions>

<Lat>0</Lat><Lng>0</Lng><Vrt>-80</Vrt><Pitch>0</Pitch>
    </Positions>
    </Mvd>
</ImagingPoint>
<ImagingPoint>
    <Cp>15</Cp>
    <Acquisition>
        <AcquisitionId>12</AcquisitionId>
        <AcquisitionSpecs />
        <AcquisitionParameters>
            <ImageMode id="Highres" />

<CalibrationSet>DefaultCalibrationSetId</CalibrationSet>
    <MV />
    </AcquisitionParameters>
</Acquisition>
<Mvd>
    <Positions>

<Lat>0</Lat><Lng>0</Lng><Vrt>-80</Vrt><Pitch>0</Pitch>
    </Positions>
    </Mvd>
</ImagingPoint>
<ImagingPoint>
    <Cp>18</Cp>
    <Acquisition>
        <AcquisitionId>13</AcquisitionId>
        <AcquisitionSpecs />
        <AcquisitionParameters>
            <ImageMode id="Highres" />

<CalibrationSet>DefaultCalibrationSetId</CalibrationSet>
    <MV />
    </AcquisitionParameters>
</Acquisition>
<Mvd>
    <Positions>

<Lat>0</Lat><Lng>0</Lng><Vrt>-80</Vrt><Pitch>0</Pitch>
    </Positions>
    </Mvd>
</ImagingPoint>
<ImagingPoint>
    <Cp>19</Cp>
    <Acquisition>
        <AcquisitionId>14</AcquisitionId>
        <AcquisitionSpecs />
        <AcquisitionParameters>
            <ImageMode id="Highres" />

<CalibrationSet>DefaultCalibrationSetId</CalibrationSet>
    <MV />
    </AcquisitionParameters>
</Acquisition>

```

```

        <Mvd>
            <Positions>
<Lat>0</Lat><Lng>0</Lng><Vrt>-80</Vrt><Pitch>0</Pitch>
                </Positions>
            </Mvd>
        </ImagingPoint>
    <ImagingPoint>
        <Cp>22</Cp>
        <Acquisition>
            <AcquisitionId>15</AcquisitionId>
            <AcquisitionSpecs />
            <AcquisitionParameters>
                <ImageMode id="Highres" />
        </Acquisition>
    </ImagingPoint>
<CalibrationSet>DefaultCalibrationSetId</CalibrationSet>
    <MV />
    </AcquisitionParameters>
</Acquisition>
<Mvd>
    <Positions>
<Lat>0</Lat><Lng>0</Lng><Vrt>-80</Vrt><Pitch>0</Pitch>
        </Positions>
    </Mvd>
</ImagingPoint>
<ImagingPoint>
    <Cp>23</Cp>
    <Acquisition>
        <AcquisitionId>16</AcquisitionId>
        <AcquisitionSpecs />
        <AcquisitionParameters>
            <ImageMode id="Highres" />
    </Acquisition>
</ImagingPoint>
<CalibrationSet>DefaultCalibrationSetId</CalibrationSet>
    <MV />
    </AcquisitionParameters>
</Acquisition>
<Mvd>
    <Positions>
<Lat>0</Lat><Lng>0</Lng><Vrt>-80</Vrt><Pitch>0</Pitch>
        </Positions>
    </Mvd>
</ImagingPoint>
<ImagingPoint>
    <Cp>26</Cp>
    <Acquisition>
        <AcquisitionId>17</AcquisitionId>
        <AcquisitionSpecs />
        <AcquisitionParameters>
            <ImageMode id="Highres" />
    </Acquisition>
</ImagingPoint>
<CalibrationSet>DefaultCalibrationSetId</CalibrationSet>
    <MV />
    </AcquisitionParameters>
</Acquisition>
<Mvd>
    <Positions>
<Lat>0</Lat><Lng>0</Lng><Vrt>-80</Vrt><Pitch>0</Pitch>
        </Positions>
    </Mvd>

```

```

        </ImagingPoint>
        <ImagingPoint>
            <Cp>27</Cp>
            <Acquisition>
                <AcquisitionId>18</AcquisitionId>
                <AcquisitionSpecs />
                <AcquisitionParameters>
                    <ImageMode id="Highres" />
            </Acquisition>
        </ImagingPoint>
        <CalibrationSet>DefaultCalibrationSetId</CalibrationSet>
            <MV />
        </AcquisitionParameters>
    </Acquisition>
    <Mvd>
        <Positions>
            <Lat>0</Lat><Lng>0</Lng><Vrt>-80</Vrt><Pitch>0</Pitch>
        </Positions>
    </Mvd>
</ImagingPoint>
<ImagingPoint>
    <Cp>30</Cp>
    <Acquisition>
        <AcquisitionId>19</AcquisitionId>
        <AcquisitionSpecs />
        <AcquisitionParameters>
            <ImageMode id="Highres" />
    </Acquisition>
</ImagingPoint>
<CalibrationSet>DefaultCalibrationSetId</CalibrationSet>
    <MV />
</AcquisitionParameters>
</Acquisition>
<Mvd>
    <Positions>
        <Lat>0</Lat><Lng>0</Lng><Vrt>-80</Vrt><Pitch>0</Pitch>
    </Positions>
</Mvd>
</ImagingPoint>
<ImagingPoint>
    <Cp>31</Cp>
    <Acquisition>
        <AcquisitionId>20</AcquisitionId>
        <AcquisitionSpecs />
        <AcquisitionParameters>
            <ImageMode id="Highres" />
    </Acquisition>
</ImagingPoint>
<CalibrationSet>DefaultCalibrationSetId</CalibrationSet>
    <MV />
</AcquisitionParameters>
</Acquisition>
<Mvd>
    <Positions>
        <Lat>0</Lat><Lng>0</Lng><Vrt>-80</Vrt><Pitch>0</Pitch>
    </Positions>
</Mvd>
</ImagingPoint>
    </ImagingPoints>
    <ImagingTolerances /> <!--mandatory, even if empty-->
</ImagingParameters>

```



```
</SetBeam>  
</VarianResearchBeam>
```

Appendix 2: The XML script from Python code for the off-isocenter automated WL test

```
<?xml version="1.0" ?>
<VarianResearchBeam SchemaVersion="1.0">
  <!--Build from python-->
  <SetBeam>
    <Id>1234</Id>
    <MLCModel>NDS120HD</MLCModel>
    <Accs/>
    <ControlPoints>
      <Cp>
        <SubBeam>
          <Seq>0</Seq>
          <Name>MV Outside</Name>
        </SubBeam>
        <Energy>6x</Energy>
        <Mu>0</Mu>
        <DRate>400</DRate>
        <GantryRtn>0.0</GantryRtn>
        <CollRtn>180</CollRtn>
        <CouchRtn>180</CouchRtn>
        <Y1>-0.0</Y1>
        <Y2>2.7</Y2>
        <X1>3.2</X1>
        <X2>3.2</X2>
        <Mlc>
          <ID>1</ID>
          <B>1.390 1.390 1.390 1.390 1.390 1.390 1.390 1.390
1.390 1.390 1.390 1.390 1.390 1.390 1.390 1.390 1.390 1.390 1.390 1.390
1.390 1.390 1.390 1.390 1.390 1.390 1.390 1.390 1.390 1.390 1.390 1.580
1.970 2.207 2.332 2.375 2.326 2.232 2.065 1.720 1.390 1.390 1.390 1.390
1.390 1.390 1.390 1.390 1.390 1.390 1.390 1.390 1.390 1.390 1.390 1.390
1.390 1.390 1.390 1.390</B>
          <A>-1.390 -1.390 -1.390 -1.390 -1.390 -1.390 -1.390 -1.390 -
1.390 -1.390 -1.390 -1.390 -1.390 -1.390 -1.390 -1.390 -1.390 -
1.390 -1.390 -1.390 -1.390 -1.390 -1.390 -1.390 -1.390 -1.390 -
1.390 -1.390 -1.390 -1.130 -0.830 -0.562 -0.437 -0.405 -0.445 -
0.542 -0.710 -0.960 -1.390 -1.390 -1.390 -1.390 -1.390 -1.390 -
1.390 -1.390 -1.390 -1.390 -1.390 -1.390 -1.390 -1.390 -1.390 -
1.390 -1.390 -1.390</A>
        </Mlc>
      </Cp>
    </Cp/>
    <Cp>
      <GantryRtn>90.0</GantryRtn>
      <Mlc>
        <ID>1</ID>
        <B>1.390 1.390 1.390 1.390 1.390 1.390 1.390 1.390
1.390 1.390 1.390 1.390 1.390 1.390 1.390 1.390 1.390 1.390 1.390
1.390 1.390 1.390 1.390 1.390 1.390 1.390 1.390 1.390 1.390 1.390
0.543 0.799 0.907 0.967 0.928 0.838 0.678 0.475 1.390 1.390 1.390 1.390
1.390 1.390 1.390 1.390 1.390 1.390 1.390 1.390 1.390 1.390 1.390
1.390 1.390 1.390 1.390</B>
```

<A>-1.390 -1.390 -1.390 -1.390 -1.390 -1.390 -1.390 -
1.390 -1.390 -1.390 -1.390 -1.390 -1.390 -1.390 -1.390 -1.390 -1.390 -
1.390 -1.390 -1.390 -1.390 -1.390 -1.390 -1.390 -1.390 -1.390 -1.390 -
1.390 -1.390 -1.390 -1.390 0.238 0.583 0.854 0.960 0.988 0.985 0.899 0.750
0.525 -1.390 -1.390 -1.390 -1.390 -1.390 -1.390 -1.390 -1.390 -1.390 -
1.390 -1.390 -1.390 -1.390 -1.390 -1.390 -1.390 -1.390 -1.390 -1.390 -
1.390

</Mlc>
</Cp>
<Cp/>
<Cp>
<GantryRtn>180.0</GantryRtn>
<Mlc>

<ID>1</ID>
1.390 1.390 1.390 1.390 1.390 1.390 1.390 1.390 1.390
1.390 1.390 1.390 1.390 1.390 1.390 1.390 1.390 1.390 1.390 1.390 1.390
1.390 1.390 1.390 1.390 1.390 1.390 1.390 1.390 1.390 1.390 1.390 -1.130 -
0.826 -0.562 -0.438 -0.405 -0.447 -0.539 -0.715 -1.000 1.390 1.390 1.390
1.390 1.390 1.390 1.390 1.390 1.390 1.390 1.390 1.390 1.390 1.390 1.390
1.390 1.390 1.390 1.390 1.390

<A>-1.390 -1.390 -1.390 -1.390 -1.390 -1.390 -1.390 -
1.390 -1.390 -1.390 -1.390 -1.390 -1.390 -1.390 -1.390 -1.390 -1.390 -
1.390 -1.390 -1.390 -1.390 -1.390 -1.390 -1.390 -1.390 -1.390 -1.390 -
1.390 -1.390 -1.390 -1.390 1.587 1.966 2.208 2.332 2.376 2.330 2.233 2.060
1.835 -1.390 -1.390 -1.390 -1.390 -1.390 -1.390 -1.390 -1.390 -1.390 -
1.390 -1.390 -1.390 -1.390 -1.390 -1.390 -1.390 -1.390 -1.390 -1.390 -
1.390

</Mlc>
</Cp>
<Cp/>
<Cp>
<GantryRtn>270.0</GantryRtn>
<Mlc>

<ID>1</ID>
1.390 1.390 1.390 1.390 1.390 1.390 1.390 1.390 1.390
1.390 1.390 1.390 1.390 1.390 1.390 1.390 1.390 1.390 1.390 1.390 1.390
1.390 1.390 1.390 1.390 1.390 1.390 1.390 1.390 1.390 1.390 1.390 1.390
1.390 1.390 1.390 1.390 1.390 1.390 1.390 1.390 1.390 1.390 1.390 1.390
1.390 1.390 1.390 1.390 1.390

<A>-1.390 -1.390 -1.390 -1.390 -1.390 -1.390 -1.390 -
1.390 -1.390 -1.390 -1.390 -1.390 -1.390 -1.390 -1.390 -1.390 -1.390 -
1.390 -1.390 -1.390 -1.390 -1.390 -1.390 -1.390 -1.390 -1.390 -1.390 -
1.390 -1.390 -1.390 -1.390 0.217 0.549 0.789 0.898 0.939 0.881 0.798 0.602
0.211 -1.390 -1.390 -1.390 -1.390 -1.390 -1.390 -1.390 -1.390 -1.390 -
1.390 -1.390 -1.390 -1.390 -1.390 -1.390 -1.390 -1.390 -1.390 -1.390 -
1.390

</Mlc>
</Cp>
<Cp/>
<Cp>
<GantryRtn>359.0</GantryRtn>
<Mlc>
<ID>1</ID>

```

        <B>1.390 1.390 1.390 1.390 1.390 1.390 1.390 1.390 1.390
1.390 1.390 1.390 1.390 1.390 1.390 1.390 1.390 1.390 1.390 1.390 1.390
1.390 1.390 1.390 1.390 1.390 1.390 1.390 1.390 1.390 1.390 1.390 1.580
1.970 2.207 2.332 2.379 2.329 2.235 2.065 1.700 1.390 1.390 1.390 1.390
1.390 1.390 1.390 1.390 1.390 1.390 1.390 1.390 1.390 1.390 1.390 1.390
1.390 1.390 1.390 1.390</B>
        <A>-1.390 -1.390 -1.390 -1.390 -1.390 -1.390 -1.390 -
1.390 -1.390 -1.390 -1.390 -1.390 -1.390 -1.390 -1.390 -1.390 -
1.390 -1.390 -1.390 -1.390 -1.390 -1.390 -1.390 -1.390 -1.390 -
1.390 -1.390 -1.390 -1.390 -1.130 -0.830 -0.562 -0.435 -0.405 -0.445 -
0.535 -0.715 -0.980 -1.390 -1.390 -1.390 -1.390 -1.390 -1.390 -
1.390 -1.390 -1.390 -1.390 -1.390 -1.390 -1.390 -1.390 -1.390 -
1.390 -1.390 -1.390</A>
    </Mlc>
    </Cp>
    <Cp/>
</ControlPoints>
<ImagingParameters>
    <OutsideTreatment>
        <MaxMu>100</MaxMu>
    </OutsideTreatment>
    <ImagingPoints>
        <ImagingPoint>
            <Cp>1</Cp>
            <Acquisition>
                <AcquisitionId>0</AcquisitionId>
                <AcquisitionSpecs/>
                <AcquisitionParameters>
                    <ImageMode id="Highres"/>
</ImagingPoint>
</ImagingPoints>
</ImagingParameters>
<CalibrationSet>DefaultCalibrationSetId</CalibrationSet>
    <MV/>
    </AcquisitionParameters>
</Acquisition>
<Mvd>
    <Positions>
        <Lat>0</Lat>
        <Lng>0</Lng>
        <Vrt>-80</Vrt>
        <Pitch>0</Pitch>
    </Positions>
</Mvd>
</ImagingPoint>
<ImagingPoint>
    <Cp>3</Cp>
    <Acquisition>
        <AcquisitionId>1</AcquisitionId>
        <AcquisitionSpecs/>
        <AcquisitionParameters>
            <ImageMode id="Highres"/>
</Acquisition>
</ImagingPoint>
</ImagingPoints>
</ImagingParameters>
<CalibrationSet>DefaultCalibrationSetId</CalibrationSet>
    <MV/>
    </AcquisitionParameters>

```

```

        </Acquisition>
        <Mvd>
            <Positions>
                <Lat>0</Lat>
                <Lng>0</Lng>
                <Vrt>-80</Vrt>
                <Pitch>0</Pitch>
            </Positions>
        </Mvd>
    </ImagingPoint>
    <ImagingPoint>
        <Cp>5</Cp>
        <Acquisition>
            <AcquisitionId>2</AcquisitionId>
            <AcquisitionSpecs/>
            <AcquisitionParameters>
                <ImageMode id="Highres"/>
        </AcquisitionParameters>
    </AcquisitionParameters>
</AcquisitionParameters>
<CalibrationSet>DefaultCalibrationSetId</CalibrationSet>
    <MV/>
    </AcquisitionParameters>
</AcquisitionParameters>
</Acquisition>
<Mvd>
    <Positions>
        <Lat>0</Lat>
        <Lng>0</Lng>
        <Vrt>-80</Vrt>
        <Pitch>0</Pitch>
    </Positions>
</Mvd>
</ImagingPoint>
<ImagingPoint>
    <Cp>7</Cp>
    <Acquisition>
        <AcquisitionId>3</AcquisitionId>
        <AcquisitionSpecs/>
        <AcquisitionParameters>
            <ImageMode id="Highres"/>
        </AcquisitionParameters>
    </AcquisitionParameters>
</AcquisitionParameters>
<CalibrationSet>DefaultCalibrationSetId</CalibrationSet>
    <MV/>
    </AcquisitionParameters>
</AcquisitionParameters>
</Acquisition>
<Mvd>
    <Positions>
        <Lat>0</Lat>
        <Lng>0</Lng>
        <Vrt>-80</Vrt>
        <Pitch>0</Pitch>
    </Positions>
</Mvd>
</ImagingPoint>
<ImagingPoint>
    <Cp>9</Cp>

```

```
<Acquisition>
  <AcquisitionId>4</AcquisitionId>
  <AcquisitionSpecs/>
  <AcquisitionParameters>
    <ImageMode id="Highres"/>
</AcquisitionParameters>
</Acquisition>
<CalibrationSet>DefaultCalibrationSetId</CalibrationSet>
  <MV/>
</CalibrationSet>
</ImagingPoint>
</ImagingPoints>
<ImagingTolerances/>
</ImagingParameters>
</SetBeam>
</VarianResearchBeam>
```

References

- [1] J. Berni, E. Hall and A. Giaccia, "Radiation oncology: a century of Achievement," *Nature Review. Cancer*, pp. 737-747, September 2004.
- [2] J. Ferlay, I. Soerjomataram, R. Dikshit, S. Eser, C. Mathers, M. Rebelo, D. M. Oarkin, D. Forman and F. Bray, "Cancer incidence and mortality worldwide: Sources, methods and major patterns in GLOBOCAN 2012," *International Journal of Cancer*, p. E359–E386, 2015.
- [3] G. Barnett, C. West, A. Dunning, R. Elliott, C. Coles, P. Pharoah and N. Burnet, "Normal tissue reactions to radiotherapy," *Nature Review. Cancer*, pp. 134-142, 2009.
- [4] F. M. Khan, *The Physics of Radiation Therapy*, Philadelphia, PA: Lippincott Williams & Wilkins, 2003.
- [5] I. A. E. A. IAEA, *Radiation Biology: A Handbook for Teachers and Students*, Vienna, Austria: IAEA, 2010.
- [6] E. Podgorsak, "Treatment Machines for External Beam Radiotherapy," in *Radiation Oncology Physics: A Handbook for Teachers and Students*, Vienna, International Atomic Energy Agency IAEA, 2012, pp. 123-160.
- [7] J. Wong, "Electronic Portal Imaging Devices (EPID)," in *Encyclopedia of Radiation Oncology*, Berlin, Springer, 2013.
- [8] P. Rowshanfarzad, C. McGarry, M. Barnes, M. Sabet and M. Ebert, "An EPID-based method for comprehensive verification of gantry, EPID and the MLC carriage positional accuracy in Varian linacs during arc treatments," *Radiation Oncology*, pp. 249-259, 2014.
- [9] S. Gao, P. Balter, P. Munro and A. Jeung, "Evaluation of IsoCal geometric calibration system for Varian linacs equipped with On-Board imager and electronic portal imaging device imaging systems.," *J Appl Clin Med Phys.*, p. 2014, 2014.
- [10] *TrueBeam Developer Mode Version 2.0 User's manual*, Varian Medical Systems, 2013.
- [11] J. Malicki, "The importance of accurate treatment planning, delivery, and dose verification," *Reports of Practical Oncology and Radiotherapy*, pp. 63-65, 13 Feb 2012.
- [12] S. Benedict, K. Yenice, D. Followil and J. Galvin, "Stereotactic body radiation therapy: The report of AAPM Task Group 101," pp. 4078-4101, August 2010.

- [13] S. Mitchael, L. David, L. Dennis, L. Wendell and P. Ervin, "AAPM Report NO. 54 Stereotactic Radiosurgery. Report of Task Group 42. Radiation Therapy," American Institute of Physics, 1995.
- [14] S. Seung, D. Larson, J. Galvin, M. Mehta and L. Potters, "American College of Radiology (ACR) and American Society for Radiation Oncology (ASTRO) Practice Guideline for the Performance of Stereotactic Radiosurgery (SRS)," *American Journal of Clinical Oncology*, pp. 310-315, 2013.
- [15] W. Lutz, K. Winston, and N. Maleki, "A system for stereotactic radiosurgery with a linear accelerator," *International Journal of Radiation Oncology*, pp. 373-381, 1988.
- [16] J. Gao and X. Liu, "Off-Isocenter Winston-Lutz Test for Stereotactic Radiosurgery/Stereotactic Body Radiotherapy," *International Journal of Medical Physics, Clinical Engineering and Radiation Oncology*, pp. 154-161, 2016.
- [17] G. Clark, R. Popple, P. Young and J. Fiveash, "Feasibility Of Single-Isocenter Volumetric Modulated Arc Radiosurgery for Treatment of Multiple Brain Metastases," *International Journal of Radiation*, pp. 296-302, 2010.
- [18] Y. Huang, K. Chin, J. Robbins, J. Kim, H. Li, H. Amro, I. Chetty, J. Gordon and S. Ryu , "Radiosurgery of multiple brain metastases with single-isocenter dynamic conformal arcs (SIDCA)," *Radiotherapy and Oncology*, p. 128–132, 2014.
- [19] G. Junfang and X. Liu, "Off-Isocenter Winston-Lutz Test for Stereotactic Radiosurgery/Stereotactic Body Radiotherapy," *International Journal of Medical Physics, Clinical Engineering and Radiation Oncology*, pp. 154-161, 2016.
- [20] J. Calvo-Ortega, M. Pozo, R. Moragues and J. Casals, "Targeting accuracy of single-isocenter intensity-modulated radiosurgery for multiple lesions," *Medical Dosimetry*, pp. 104-110, 2017.
- [21] I. A. E. A. IAEA, "Quality Assurance in Radiotherapy," International Atomic Energy Agency IAEA, Vienna, 1995.
- [22] D. Shepard and T. Solberg, "Quality Assurance in Stereotactic Radiosurgery and Fractionated Stereotactic Radiotherapy," in *AAPM 51st Annual Meeting*, Anaheim, California, 2009.
- [23] G. Valdes, O. Morin, J. Pouliot and C. Chuang, "SU-E-T-48: Automated Quality Assurance for XML Controlled Linacs," *Medical Physics*, p. 232, 2014.
- [24] M. Kovac, M. Iseli, S. Lang, m. Malla and C. Winter, "Six Degree of Freedom Robotic Correction Table: Integration Into Routine Radiotherapy Practice," in *ESTRO*, Barcelona, Spain, 2012.

- [25] J. Kerns, "Pylinac Winston-Lutz module documentation," Pylinac, 2017. [Online]. Available: http://pylinac.readthedocs.io/en/latest/winston_lutz.html. [Accessed 7 2017].
- [26] M. M. D. Inc., "Modus QA," 2018. [Online]. Available: <https://modusqa.com/igrt/isocenter-cube>. [Accessed 3 2018].
- [27] ModusQA, "Modus Medical Devices Inc.," 2018. [Online]. Available: <https://modusqa.com/igrt/isocenter-cube>. [Accessed 1 2018].

Curriculum Vitae

Mahmoud Yaqoub, M.Sc.

m.yaqoub@yahoo.com

Education

University of Nevada at Las Vegas, La Vegas, Nevada.

Master of Science in Medical Physics (CAMPEP accredit), 5/2018

Thesis: “Design & Delivery of Automated Winston-Lutz Test for Isocentric & Off-Axis Delivery Stability Utilizing TrueBeam Developer Mode & Electronic Portal Imaging Device”

Northern Illinois University, DeKalb, Illinois.

Master of Science in Electrical Engineering (Emphasis in Biomedical Engineering),

7/2016

Thesis: “Study of Acoustic Shadow Moiré for Imaging Technique”

Texas Tech University, Lubbock, Texas.

Master of Science in Applied physics (Emphasis in Medical Physics), 8/2013

Report: “A Study of Proton Range Variations Resulting from Changes in Relative Proton Stopping Powers for Proton Beam Therapy”

Jordan University of Science and Technology, Irbid, Jordan.

Bachelor of Science in applied physics (Emphasis in Nuclear and Radiation Techniques),
6/2001